Mixed Valence Copper(cu)/silica Nanocomposite: Synthesis, Characterization And Systematic Antimicrobial Studies

2013

Mikaeel Young
University of Central Florida

MIXED VALENCE COPPER (CU)/SILICA NANOCOMPOSITE: SYNTHESIS, CHARACTERIZATION AND SYSTEMATIC ANTIMICROBIAL STUDIES

by:

MIKAEEL YOUNG
B.Sc. University of the West Indies, 2011

A thesis submitted in fulfillment of the requirements
for the degree of Master of Science
in the Department of Molecular Biology and Microbiology
in the Burnett School of Biomedical Science
in the College of Medicine
at University of Central Florida
Orlando, Florida

Summer Term
2013

Major Professor: Swadeshmukul Santra

ABSTRACT

Copper (Cu) compounds are widely used as effective agricultural bactericides. Continuous use of these materials has led to Cu accumulation in soil over time. The United States Environmental Protection Agency (US EPA) is concerned about potential Cu contamination in the environment. Improving biocidal efficacy of Cu is an attractive alternative, allowing reduction of Cu amount per application. In this research, we focused on making water-soluble mixed-valence Copper/Silica composite nanogel (CuSiNG) material. The objective is to improve the efficacy of Cu by manipulating Cu valence states. It has been shown in the literature that Cu (0) and Cu (I) states are more potent that Cu (II) states in terms of their antimicrobial efficacy. It is hypothesized that mixed valence Cu will exhibit improved efficacy over Cu (II). A water-soluble mixed valence Cu/silica nanogel (MV-CuSiNG) composite has been synthesized and characterized. Structure, morphology, crystallinity and composition of the MV-CuSiNG material was characterized using High-Resolution Transmission Electron Microscopy (HRTEM), HRTEM Selected Area Electron Diffraction (SAED) and X-ray Photoelectron Spectroscopy (XPS). Amount of Cu loading in MV-CuSiNG composite material was estimated by Atomic Absorption Spectroscopy (AAS). To confirm presence of Cu (I) in the MV-CuSiNG material, Neocuproine (Nc, a Cu (I) specific chelator) assay was used. Antimicrobial efficacy of MV-CuSiNG and CuSiNG was evaluated against *X.alfalfae, B.subtilis* and *E.coli* using Kocide® 3000 ("Insoluble Cu (II)" compound), Copper sulfate ("Soluble Cu (II)" compound) and Cuprous chloride (Copper (I) compound) as positive controls and silica "seed" particles (without Cu loading) as negative control. Antimicrobial studies included observing bacterial growth inhibition and determining the Minimum Inhibitory Concentration (MIC). Improved antimicrobial efficacy was observed in MV-CuSiNG when compared to CuSiNG and other controls. For the assessment of plant safety of MV-CuSiNG and CuSiNG materials, phytotoxicity studies were conducted using *Vinca sp* and *Hamlin orange* under environmental conditions. It was observed that MV-CuSiNG material was safe to plants at commercially used (standard) spray application rate.

Keywords: Copper, Silica, Antimicrobial, Mixed-Valence, Nanogel, Biocide, Neocuproine

I dedicate this work to my family and friends, especially my parents (Emmanuel and Taslima), along with my sister Marissa, my brother-in-law Lester and my brothers Marc and Abdul-Azeem, without whom I would not be where I am today.

ACKNOWLEDGMENTS

I would first and foremost like to offer my sincerest gratitude to my professor Dr. Swadeshmukul Santra, for his dedicated assistance in teaching and supporting me in my research.

I warmly acknowledge my committee members Dr. William Self and Dr. Sean Moore for their continuing advice and suggestions for improving my work.

I would like to recognize Dr. Helge Heinrich, Kirk Scammon and the personnel of the Materials Characterization Facility (MCF) in the Advanced Materials Processing and Analysis Center (AMPAC) at the University of Central Florida for their assistance in conducting X-Ray Photoelectron Spectroscopy and High-Resolution Transmission Electron Microscopy. Dr. Mathew Rex of the Chemistry Department is thanked for his assistance and training with Atomic Absorption Spectroscopy. Veronica Maxwell and Lisa Sorrentino of the UCF Microbiology prep-room are thanked for their assistance in obtaining select bacterial cultures. Ernest Gemeinhart is thanked for his assistance in designing and constructing the mini-greenhouse used in phytotoxicity studies. Dr. Sean Moore and Anusha Naganathan are strongly thanked for allowing me the use of their microplate reader.

I sincerely thank my colleagues/friends Maria Ferdinand, Rishi Ramroopsingh, Nickisha Pierre-Pierre, Megan Berroth, Joshua Bazata, Pavithra Maniprasad, Srijita Basumallick and particularly Jeremy Tharkur, my sanity was maintained during this last year because of you guys. Ernest Gemeinhart, Diane Maldonado, Ushaben Lal, Mari Pina and the rest of staff of the NanoScience Technology Center are thanked for their assistance and support in my research.

I express immense gratitude to my uncles, aunts and cousins who have given me never-ending support and motivation.

I would like to thank my friends Kambiri, Keisha, Josef, Giselle, Johanna, Terrence, Romel, Khadijah, Jeselle, Sami, Leidy, Alisha, Robert, Simeon, Bracken, Khadijah, Micheal, Camilla, Anthony and Kervin for their encouragement and inspiration.

TABLE OF CONTENTS

LIST OF FIGURES

LIST OF TABLES

CHAPTER 1-INTRODUCTION

1.1 Copper

Copper is a metallic element with high thermal and conductive properties and an atomic number of 29. It is a micronutrient essential in most forms of life including humans[1]. Copper exists in 3 oxidation states (0, +1 and +2) and has been in use by mankind for thousands of years. Early usage included pigments made from Cu (II) salts of blue and green color, eventually being used as a metal in tools and weapons creating the copper age. As civilization developed further, copper was incorporated into alloys such as bronze, made up of copper and tin leading to the bronze age.

1.2 Antimicrobial Copper

Early in its usage, copper's antimicrobial properties were discovered and exploited, for uses including water storage. As time progressed, copper's antimicrobial properties were used in new and more imaginative ways, including coatings, medicines, fungicides and antifouling paints [2-5]. One of the major uses of copper in present civilization is as a bactericide/fungicide. Copper's use as a fungicide/bactericide is derived from a multiple mechanisms of toxicity.

Toxicity of copper to microorganisms has been correlated to DNA and RNA degradation, compromising cell membrane integrity and producing reactive oxygen species (ROS) [1]. Cell membrane integrity is partly contained by membrane potential and disruption of these potential have shown tendencies to cause fracturing and breaking of cell membrane [6]. Bacteria viability

has been to shown to be decreased in the case of protein inactivation via thiol interaction and radical induced base modification [7-10].

Reactive oxygen species (ROS) have been implicated as a crucial cause of bacterial cell death, including superoxide, hydrogen peroxide and the hydroxyl radical [11, 12] . The hydroxyl radical ($OH^{\cdot}$**)** is considered the most reactive and toxic of ROS. Its production was first described in the Fenton reaction [10]. The Fenton reaction involved the use of the element Fe as the catalysis for radical production. A Cu version of the Fenton Reaction was eventually created known as the Haber-Weiss reaction [13]. It seen that Cu (I) plays a bigger role in radical production than Cu (II) and maybe key to increasing radical production.

$$H_2O_2 + O_2^- \text{----->} O_2 + OH^- + OH^{\cdot} \quad \textbf{[13]}$$

$$Cu\ (II) + O_2^- \text{-----> } Cu\ (I) + O_2$$

$$Cu\ (I) + H_2O_2 \text{----- > } Cu\ (II) + O_2 + OH^- + OH^{\cdot}$$

Cu (I) has been shown to damage various protein families by liganding to coordinating sulfur atoms [14]. Many Cu resistance mechanisms have been discovered to involve the removal of Cu (I), such as the transport of Cu (I) ions from the cytoplasm to the periplasm and then onto the extracellular space [15-18]. This points towards Cu (I) ions' higher toxicity than Cu (II) ions.

1.3 Citrus canker and copper

The citrus industry in Florida has long been a significant part of the state economy. The industry directly or indirectly employs over 100,000 individuals and is worth billions of dollars. Citrus canker is disease of concern in Florida which causes early fruit drop and lesions to develop on leaves and fruits. While lesions pose no danger to humans, the fruit is considered undesirable and leads to losses in crop yield and sales. The disease is caused by *Xanthomonas axonopodis pv citri*, a rod shaped gram negative bacterium. Copper formulations have been shown to be successful at preventing canker infection keeping the disease under control [19-21].

While current Cu formulations have shown the ability to protect against some plant pathogens, the dosage and frequency of applications is high. Extensive use of these formulations has led to accumulation of Cu in soils. Cu accumulation not only endangers non-target microorganisms but also can lead to plant damage. Plant tissue damage due to copper exposure is caused by a variety of mechanisms including ROS production. Different species exhibit different levels of tolerance to copper induced ROS occurrences and activate stress responses [22, 23]. Many technologies are in development to remediate and reduce Cu pollution in soils but they are expensive and not feasible at this time [24-26]. Due to the potential danger of copper toxicity on plants and accumulation in the environment, it is important to use the least amount of Cu while still maintaining adequate protection against plant based pathogens.

1.4 Silica and Silica nanomaterials

Silicon is a mineral of high abundance on Earth. It exhibits a variety of properties making it suitable for many applications. It is non-flammable, stable and non-toxic. As a host matrix, it is easy to modify, use and maintain. These properties have led to silica use in fluorescent biomarkers and aerogels [27-29]. Copper silica nanoparticles have been found to be very effective at preventing bacterial growth. Loading of copper into a silica matrix allows for slower copper release and hence lower copper environmental accumulation[30].

1.5 Copper Silica Nanogel Materials

Copper silica nanomaterials are increasingly being created and used. As copper is a cheap and abundant antimicrobial agent, uses have included surface coatings and odor removal [4, 31-33]. The present study will attempt to synthesize a copper silica nanogel with high Cu loading while keeping the procedure simple and industrially feasible. With the purpose to creating an effective and low Cu content formula, the Cu (I) content of the nanogel will be manipulated and increased in an attempt to improve the bactericidal effects. Improving the efficacy of Cu at lower concentrations is crucial to reducing the accumulation of Cu in the environment and eventually to remove it.

CHAPTER 2- MATERIALS AND METHODOLOGY

2.1 Materials

All reagents used in synthesis and studies were purchased from commercial vendors and utilized without any further purification. Tetraethylorthosilicate (TEOS, Gelest Inc.), Copper Sulfate Pentahydrate (CQ concepts, Ringwood, IL), Ethylenediaminetetraacetic acid (EDTA, Amresco Inc.), ethanol (95%) (Pharmco-Aaper) Concentrated Hydrochloric Acid (Fisher Scientific), Methanol (Fisher Scientific), Zinc powder (Fisher Scientific), Sodium Borohydride (Sigma-Aldrich), Neocuproine (Acros), D-Mannitol (Acros), N,N'-Dimethylthiourea (Acros), Deionized water (Nanopure; Barnstead Model # D11911). Kocide® 3000, a product of DuPont was received as a gift from Dr. Jim Graham (Citrus Research and Education Center, Lake Alfred, FL). Luria Bertani (LB) broth and agar as well as Muller Hinton 2 (MH2) broth and agar were purchased from Fluka. Trypic Soy (TS) agar was purchased from Himedia while Tryptic Soy (TS) broth was purchased from MP Biomedicals. *B.subtilis* strain ATCC 9372 and *E.coli* strain ATCC 35218 were obtained from the Microbiology Lab at the University of Central Florida. *X.alfalfae* strain ATCC 49120 was purchased from ATCC with a permit from the U.S Department of Agriculture.

2.2 Instrumentation

Copper loading into the silica nanogel was confirmed using Atomic Absorption Spectroscopy (AAS) using a Perkin Elmer Analyst 400 AA flame spectrometer and a Cary Win UV-Vis Spectrometer. Nanogel dispersion, surface morphology and crystallinity was observed using a FEI Tecnai F30 TEM. Valence states of copper were analyzed using a Physical Electronics 5400 ESCA (XPS) spectrometer. Bacterial growth inhibition assays were recorded using a Biotek Mx microplate reader.

2.3 Methodology

2.3.1 Synthesis of Nanocomposite Materials

2.3.1.1 Synthesis of Copper-Silica Nanogel 4

The Copper Silica Nanogel (CuSiNG) 4 material was synthesized using an acid hydrolysis protocol [34]. Using a measuring cylinder, 110 mL of nanopure deionized water was first acidified by addition of 330 µL 1% hydrochloric acid (made from concentrated hydrochloric acid). Following this, 1.87 g of copper sulfate pentahydrate was added and dissolved while stirring. Finally, 778 µL tetraethylorthosilicate (TEOS) was added drop-wise to the mixture which was left to stir for 24 hrs. The pH of the nanogel was checked using a Mettler Toledo pH meter and determined to be 4.

2.3.1.2 Synthesis of Mixed Valence Copper-Silica Nanogel B

CuSiNG 4 was prepared as stated above. While continuing with stirring, 330 mg of zinc powder was added to the mixture. The mixture was left to stir for 1 hr. After the set time period was ended, the mixture was separated and centrifuged at 10,000 rpm for 10 minutes to remove un-reacted residue. The pH of the nanogel was checked using a Mettler Toledo pH meter and determined to be 4. The nanogel was named B since it was the most successful trial among a series of trials (A, B, C and D), using different nanogel copper to zinc ratios.

2.3.1.3 Synthesis of Mixed Valence Copper-Silica Nanogel S

CuSiNG 4 was prepared as stated above. While continuing with stirring, 183.3 mg of sodium borohydride was added to the mixture. The mixture was left to stir for 1 hr. After the set time period ended, the mixture was separated and centrifuged at 10,000 rpm for 10 minutes to remove un-reacted residue. The pH of the nanogel was checked using a Mettler Toledo pH meter and determined to be 4. The nanogel was named S from the use of sodium borohydride.

2.3.2 Nanogel Characterization

Copper loaded Silica 4, B and S nanogels were characterized using a variety of techniques including Atomic Absorption Spectroscopy (AAS), Transmission Electron Microscopy (TEM), X-ray Photoelectron Spectroscopy (XPS), and UV-Vis Spectroscopy.

2.3.2.1 Atomic Absorption Spectroscopy

Samples for AAS were prepared by lyophilizing 10 mL of each nanogel and extracting the Cu using a saturated ethylenediaminetetraacetic acid (EDTA) solution. A second AAS measurement was taken using an acidified EDTA solution for comparison. EDTA leeches out the Cu to form the water soluble Cu-EDTA complex [24]. AAS analysis was done by comparing nanogel samples with a series of copper standards.

2.3.2.2 Transmission Electron Microscopy

Sample preparation for TEM was carried out by dipping carbon filmed gold (Au) grids ((400 square mesh), Electron Microscope Sciences) in the respective nanogels and allowed to dry in a desiccator. Grids were carried over to UCF-AMPAC-MCF for analysis. Use of the TEM was executed by MCF personnel. Electron beam intensity of 100 KV was used for TEM. Energy-dispersive X-ray spectroscopy, low resolution spectra, high resolution spectra, and selected area electron diffraction data were collected for each CuSiNG material and analyzed using Digital Micrograph software.

2.3.2.3 X-ray Photoelectron Spectroscopy

10 mL of each nanogel was frozen in a 15 mL microcentrifuge tube and lyophilized (LabConco FreeZone 4.5 Liter Freeze Dry System Model 7750020). The lyophized powder was collected and carried over to UCF-AMPAC-MCF for analysis. Sample was loaded into the XPS

spectrometer by MCF personnel and scanning was carried out under MCF personnel supervision. Survey and high resolution spectra were collected for all 3 nanogels. Copper valence information was analyzed by AugerScan software, identifying Cu compounds using the National Institute of Standards and Technology (NIST) XPS database.

2.3.2.4 UV-Vis Spectroscopy

Copper (I) content within CuSiNG materials was observed using 2, 9-dimethyl-1, 10-phenanthroline (Neocuproine) (N_c) with UV-Vis spectroscopy. Nc is a copper (I) specific chelator, soluble in methanol and chloroform. The Cu (I)-Nc complex has been shown to absorb with peak maximums at 450-460 nm [35-39]. Nc was solubilized in methanol (1mg/mL) and added to equal concentrations of CuSiNG materials and placed on a stir plate for 36-48 hrs. After stirring, UV-Vis spectra between 350-550 nm were obtained for all mixtures using equal dilutions.

2.3.3 Antimicrobial Studies

The antimicrobial properties of CuSiNG materials were investigated using a range of techniques including Minimum Inhibitory Concentration (MIC), Disk Diffusion, Bacterial Growth Inhibition Assay and Hydroxyl Radical Scavenging Assay. CuSiNG 4, B and S were tested against gram negative *Xanthomonas alfalfae* subsp. *Citrumelonis* (*X.alfalfae,* ATCC

49120), gram negative *Escherichia coli* (*E.coli*, ATCC 35218) and gram positive *Bacillus subtilis* (*B.subtilis*, ATCC 9372) organisms. All bacteria were obtained from American Type Culture Collection *(*ATCC*)* and UCF Department of Molecular Biology and Microbiology Preparatory Laboratory, University of Central Florida, Orlando, FL. *E.coli* and *B.subtilis* were sub-cultured and maintained using LB agar and broth while *X.alfalfae* was subcultured and maintained using TS agar and broth. Culturing and testing against *X.alfalfae* was carried out at 31^{o}C while *E.coli* and *B.subtilis* cultures and tests were conducted at 37^{o}C. All antimicrobial studies were conducted using MH2 agar and broth with bacterial concentrations of 0.5 McFarland Standard (10^{8} CFU/mL). CuSiNG 4, B and S were compared to Kocide® 3000 ("Insoluble Cu (II)" compound), Copper Sulfate ("Soluble Cu (II)" compound) and Cuprous chloride (Copper (I) control) as positive controls and silica nanogel (no Cu loaded) as a negative control.

2.3.3.1 Disk Diffusion

Disk diffusion assays were carried out using blank disks (Remel, Thermo Scientific). Blank disks were soaked in 5 mL of the testing solution (CuSiNG 4, CuSiNG B, CuSiNG S $CuSO_4$, CuCl, Kocide® 3000 and SiNG) on a shaker at 150 rpm for 3-4 hrs. After soaking, disks were dried overnight at room temperature. MH2 agar plates were prepared and a "lawn" of each appropriate bacterium was streaked. Disks were placed on the streaked plates using forceps and incubated inverted for 20-24 hrs at the appropriate temperatures. After incubation, zones of inhibition were measured in mm.

2.3.3.2 Bacterial Growth Inhibition

The bacterial growth inhibition studies for the CuSiNG 4, B and S were conducted using a modified version of the method described by Rastogi et al[40]. The procedure is briefly described below. Different volumes of CuSiNG 4, B and S (Cu content: 43.27µg, 56.25µg, 69.23µg, 82.21µg, 95.19µg and 108.18µg) were prepared in sterile MH2 broth in separate wells within a 96-well microplate. Uniform growth potential was ensured by each well containing equal amounts of broth and equal final volumes (250 µL). Each well contained 20 µL of bacteria (10^8 CFU). Appropriate "blank" wells were prepared containing no bacteria in order to compare with samples to determine bacterial growth. Microplates were incubated at the appropriate temperature for each bacterial species on a shaker at 150 rpm for 20-24hrs. After the allotted time, the turbidity (optical density, OD) of the wells was determined by measuring the absorbance at 600 nm with a microplate reader. Bacterial growth was determined by subtracting the OD of the blanks from the OD of the sample wells to reveal the specific bacterial OD. The bacterial OD was taken as a measure of growth and graphed to compare with controls.

In addition to performing growth inhibition assays on *X.alfafae, B.subtilis* and *E.coli*, a copA1*E.coli* mutant was used to ascertain whether Cu (I) did play a large role in Cu toxicity. CopA is known as the gene responsible for the development of Cu (I) efflux pumps which translocates Cu (I) from the cytoplasm to periplasm when the Cu (I) concentration gets too high [16].

2.3.3.3 Minimum Inhibitory Concentration (MIC)

The Minimum Inhibitory Concentration (MIC) of CuSiNG 4, B and S were determined along with Kocide® 3000 ("Insoluble Cu (II)" compound), Copper sulfate ("Soluble Cu (II)" compound) and Cuprous chloride (Copper (I) control) with equivalent Cu concentrations. MIC testing was carried out using broth microdilution in accordance with the guidelines of the Clinical and Laboratory Standards Institute (CLSI) [41].

2.3.3.4 Hydroxyl Radical Scavenging

Hydroxyl radical activity was observed by adding hydroxyl radical scavengers to the bacterial growth inhibition assays with selected Cu contents (43.27µg, 69.23µg and 95.19µg). The hydroxyl radical scavengers D-Mannitol (MW=182.17) and N,N'-Dimethylthiourea (MW=104.18) were chosen due to their well known use in ROS experiments [10, 42-44]. D-Mannitol and N,N'-Dimethylthiourea were solubilized in DI-water to make stock solutions of 1 mM concentration. A well concentration of 100 µM was achieved by adding 25 µL of the 1 mM solution to each well with final volumes of 250 µL (1:10 dilution) after scavenger addition. The effects of hydroxyl radicals on the viability of bacteria in the presence of Cu were investigated by comparing bacterial OD after Cu exposure with and without scavengers present.

2.3.4 Phytotoxicity Studies

Phytotoxicity studies of CuSiNG materials and controls were carried out to observe potential plant tissue damage. Studies were conducted using *Vinca sp*, an annual ornamental plant purchased from Home Depot and *Hamlin orange*, a citrus species purchased from Lukas Nursery in Oviedo, FL. Studies were carried out in a polyvinyl chloride (PVC) cold frame "mini greenhouse" covered in shade cloth and equipped with an Acurite® temperature and humidity sensor purchased from Home Depot. Plants were purchased and placed in the greenhouse at least 24 hrs prior to application of the formulation, allowing for acclimatization. Weather and conditions were monitored to ensure that plants were only sprayed on appropriate days for phytotoxicity (Temperature >80 F, Humidity 60-80%). CuSiNG 4, B and S were applied, along with Kocide® 3000 ("Insoluble Cu (II)" compound), Copper sulfate ("Soluble Cu (II)" compound) and Cuprous chloride (Copper (I) compound) and SiNG (no Copper loaded) used for comparisons. Formulations were sprayed at concentrations 90, 450 and 900 ppm at 8AM and observations were taken at 24, 48 and 72 hr time points.

CHAPTER 3- RESULTS AND DISCUSSION

3.1 Synthesis of Nanocomposite Materials

Copper Silica Nanogel (CuSiNG) 4 was successfully synthesized as described above. The nanogel was blue in color and transparent (**Figure 1**). CuSiNG 4 exhibited prolonged shelf life with stable samples lasting at least 12 months. CuSiNG B was successfully synthesized with a pale blue color, transparency, and high stability (**Figure 2**). CuSiNG S exhibited similar characteristics as CuSiNG 4, with a light blue color, transparency and prolonged stability (**Figure 3**).

3.2 Nanogel Characterization

Copper loading into CuSiNG was confirmed and measured using Atomic Absorption Spectroscopy (AAS). Analysis of Cu samples compared to Cu standards revealed metallic Cu content was 4327 µg/ mL (ppm) for CuSiNG 4, 4293 µg/ mL (ppm) for CuSiNG B and 4278 µg/ mL (ppm) for CuSiNG S. Using acidified EDTA, the values obtained were 4179 µg/ mL (ppm) for CuSiNG 4, 4122 µg/ mL (ppm) for CuSiNG B and 4181 µg/ mL (ppm) for CuSiNG S.

Transmission Electron Microscopy (TEM) was used to observe nanogel dispersion and crystallinity. Elemental mapping and confirmation was analyzed using Energy-dispersive X-ray spectroscopy (EDX), indicating the presence of Cu, Si, S, O and Au (TEM grid) (**Figures 4, 8**

and 12). Low resolution images were taken of CuSiNG 4, B and S demonstrating the presence of electron rich material seen as dark contrast (**Figures 5, 9 and 13**). High resolution images confirmed the crystalline nature of the copper within CuSiNG 4, B and S with crystallites between ~4-8 nm in size being observed. Lattice spacing was calculated to reveal Cu crystallites of cupric oxide, cuprous oxide and metallic Cu in CuSiNG 4, B and S (**Figures 6, 10 and 14**). Selected area electron diffraction (SAED) of CuSiNG 4, B and S signified the amorphous nature of the silica matrix and crystallinity of Cu materials (**Figures 7, 11 and 15**)

Copper valence states were analyzed using X-ray photoelectron spectroscopy (XPS). Survey spectra were collected for CuSiNG 4, B and S to confirm elemental mapping showing the presence of Cu, Si, S, O, C and Cl (**Figures 16, 18 and 20**). High resolution spectra of Cu within CuSiNG 4, B and S was carried out to identify the Cu compounds with the nanogels (**Figures 17, 19 and 21**). Curve fitting and referencing through the National Institute for Science and Technology (NIST) XPS database indicated the Cu compounds were $CuSO_4$, $CuCl_2$, CuO, Cu_2O and metallic Cu. Copper (II) compounds were the major compounds found in all 3 CuSiNG materials; however CuSiNG B and S demonstrated a higher intensity of Cu (I) compounds as compared to CuSiNG 4, confirming the creation of a Cu mixed valence system.

Presence of Cu (I) in CuSiNG 4, B and S was confirmed and compared using Nc, a Cu (I) specific chelator. The Cu (I)-Nc complex shows an absorption maximum around ~450-460 nm [35-39]. It was seen that Nc, MeOH (solvent), $CuSO_4$, CuCl, CuSiNG 4, B and S alone do not have any peaks at ~450-460 nm. Nc-$CuSO_4$ and Nc-CuSiNG 4 had very small, negligible peaks at 455 nm while Nc-CuCl demonstrated a significant peak at 455 nm. Nc-CuSiNG B and Nc-CuSiNG S shows moderate peaks, higher than Nc-$CuSO_4$ and Nc-CuSiNG 4 but lower than Nc-

CuCl at 455 nm **(Figure 22)**. Metallic Cu content was kept equal before exposure to Nc, therefore indicating that CuSiNG B and S had higher Cu (I) content compared to CuSiNG 4.

3.3 Antimicrobial Studies

Various antimicrobial assays were performed to measure the effectiveness of CuSiNG materials at inhibiting bacterial growth and/or causing bacterial cell death.

Disk Diffusion assays were conducted as part of the antimicrobial studies. Due to limited motility of Cu within agar, the results could not be used to fully compare tests samples. The results still showed general satisfactory antimicrobial efficacy (**Figures 23, 24, 25 and Table 1**).

Growth inhibition assays were performed on *X.alfalfae* (**Figures 26 and 27**), *B.subtilis* (**Figures 28 and 29**), *E.coli* (**Figures 30 and 31**) and *E.coliΔcopA1(del)* (**Figures 32 and 33**). In general, CuSiNG B and CuSiNG S exhibited improved antimicrobial efficacy over CuSiNG 4, indicating that a mixed valence Cu system would be better at inhibiting bacterial growth than a Cu (II) only system. CuSiNG materials performed better than controls with all bacteria samples. *E.coliΔcopA1(del)* was far more susceptible to the Cu material than regular *E.coli*, confirming the significant role Cu (I) plays in Cu mechanisms of action.

MIC results reinforced and confirmed hypothesis that mixed valence CuSiNG formulas were more efficient than Cu (II) only systems (**Table 2**).

3.4 Hydroxyl Radical Scavenging

Growth inhibition assays were carried out in *E.coli* in the presence and absence of hydroxyl radical scavengers to indirectly confirm the presence of radical formation. Both D-Mannitol (**Figures 34 and 35**) and N,N'-Dimethylthiourea (**Figures 36 and 37**) assays indicated that the bacteria survived better in the presence of the hydroxyl radical scavengers. This would suggest that hydroxyl radicals were produced as part of the mechanism of action of Cu toxicity.

3.5 Phytotoxicity Studies

Plant tissue damage was tested on *Hamlin orange* and *Vinca sp.* in order to observe their levels of tolerance to copper toxicity. *Hamlin orange* was tested as a model citrus species while *Vinca sp*. is a widely known ornamental species. *Hamlin orange* exhibited strong tolerance to potential copper toxicity and showed zero plant tissue damage even at the highest (900 ppm) Cu concentrations for all formulations after three days (**Table 3 and Figure 38**). This indicates that *Hamlin orange* and other potential citrus species, in general, have strong response mechanisms allowing them to withstand copper toxicity [23]. Vinca sp. exhibited moderate to high levels of plant tissue damage when exposed to copper nanomaterials. Plant tissue damage was seen for all copper formulations with the exception of Kocide 3000. All formulations showed no damage at 90 ppm but caused moderate to serious damage at 900 ppm (**Table 4 and Figure 39**). This could be related to the solubility of the copper formulations and the readiness of free copper ions being released. Kocide 3000 is created using copper hydroxide which has a lower solubility than copper sulfate.

Figure 1: Copper Silica Nanogel pH 4

Figure 2: Mixed Valence Copper Silica Nanogel B

Figure 3: Mixed Valence Copper Silica Nanogel S

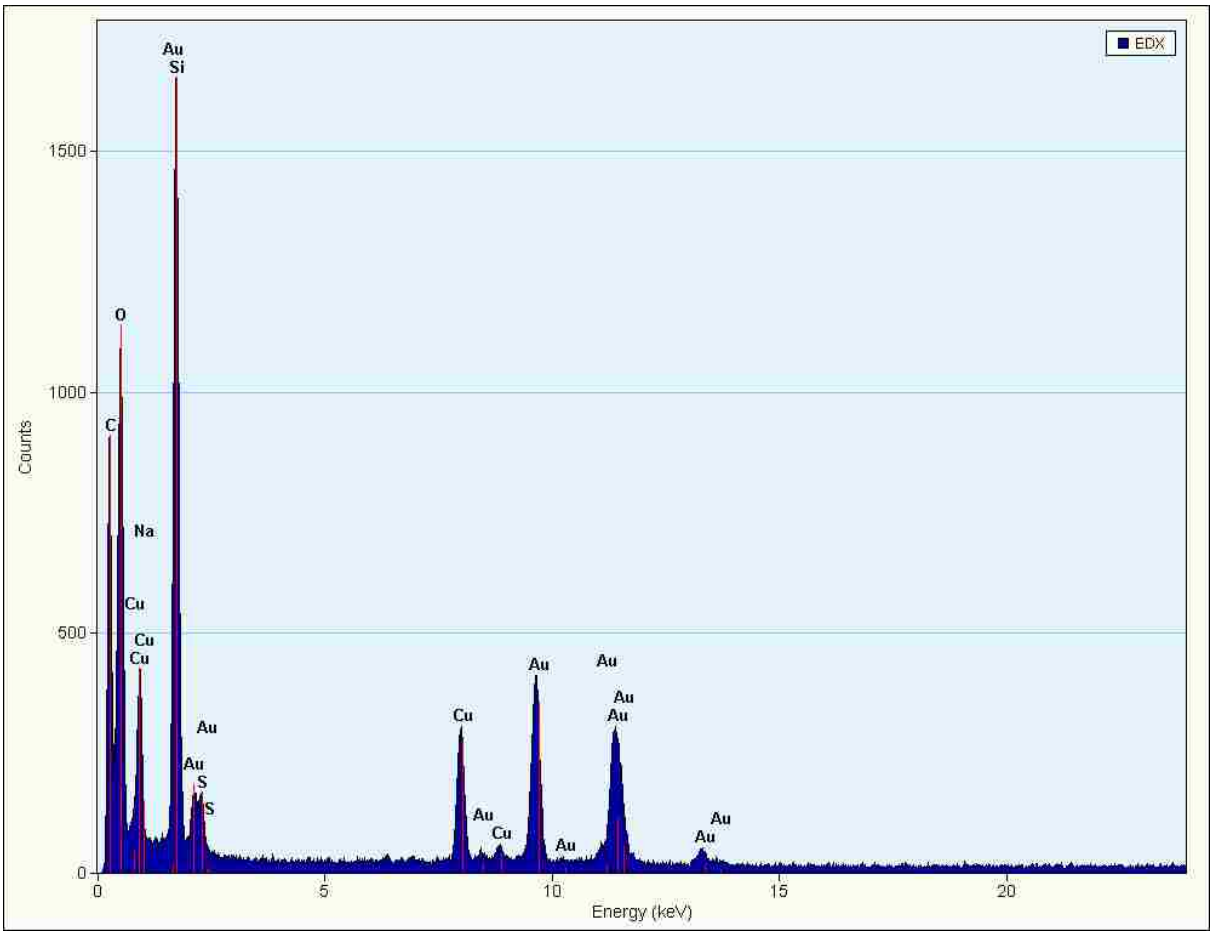

Figure 4: Energy-dispersive X-ray spectroscopy (EDX) for elemental analysis of CuSiNG 4 during HR-TEM.

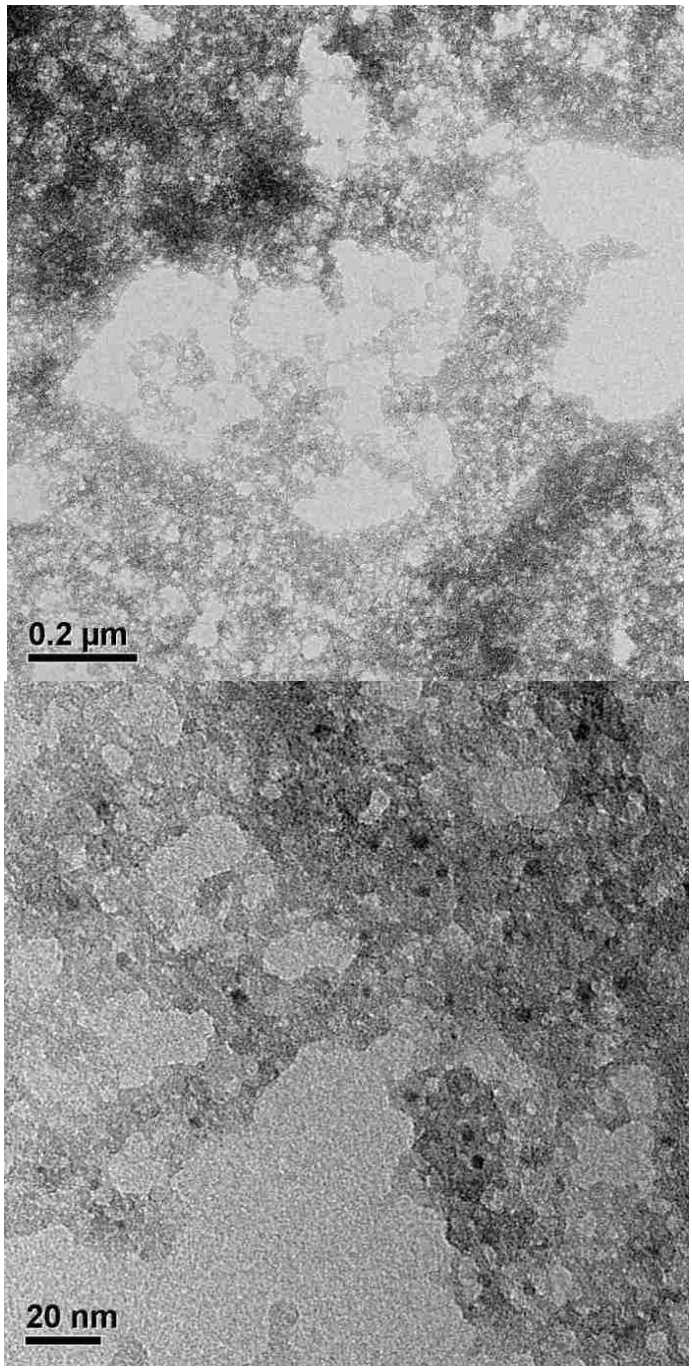

Figure 5: HR-TEM (low magnification) image of CuSiNG 4 with scattered dark contrast confirming presence of electron-rich material.

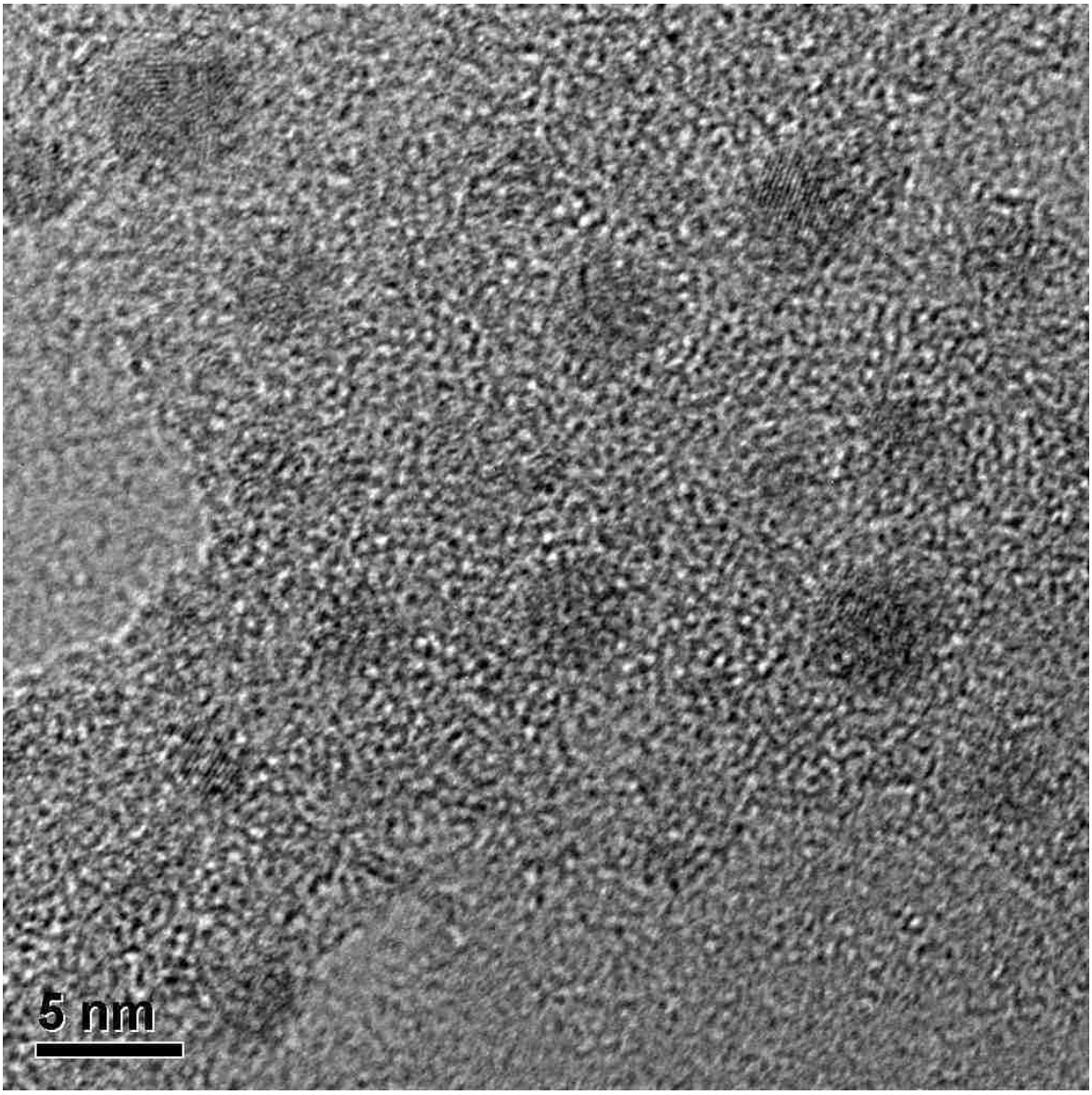

Figure 6: HR-TEM images of CuSiNG 4 with scattered dark contrast confirming presence of electron-rich material (circled in yellow). Lattice spacing measured from enlarged HR-TEM (Inset) is ~ 1.87 Å, ~2.32 Å, ~2.47 Å and ~3.02 Å.

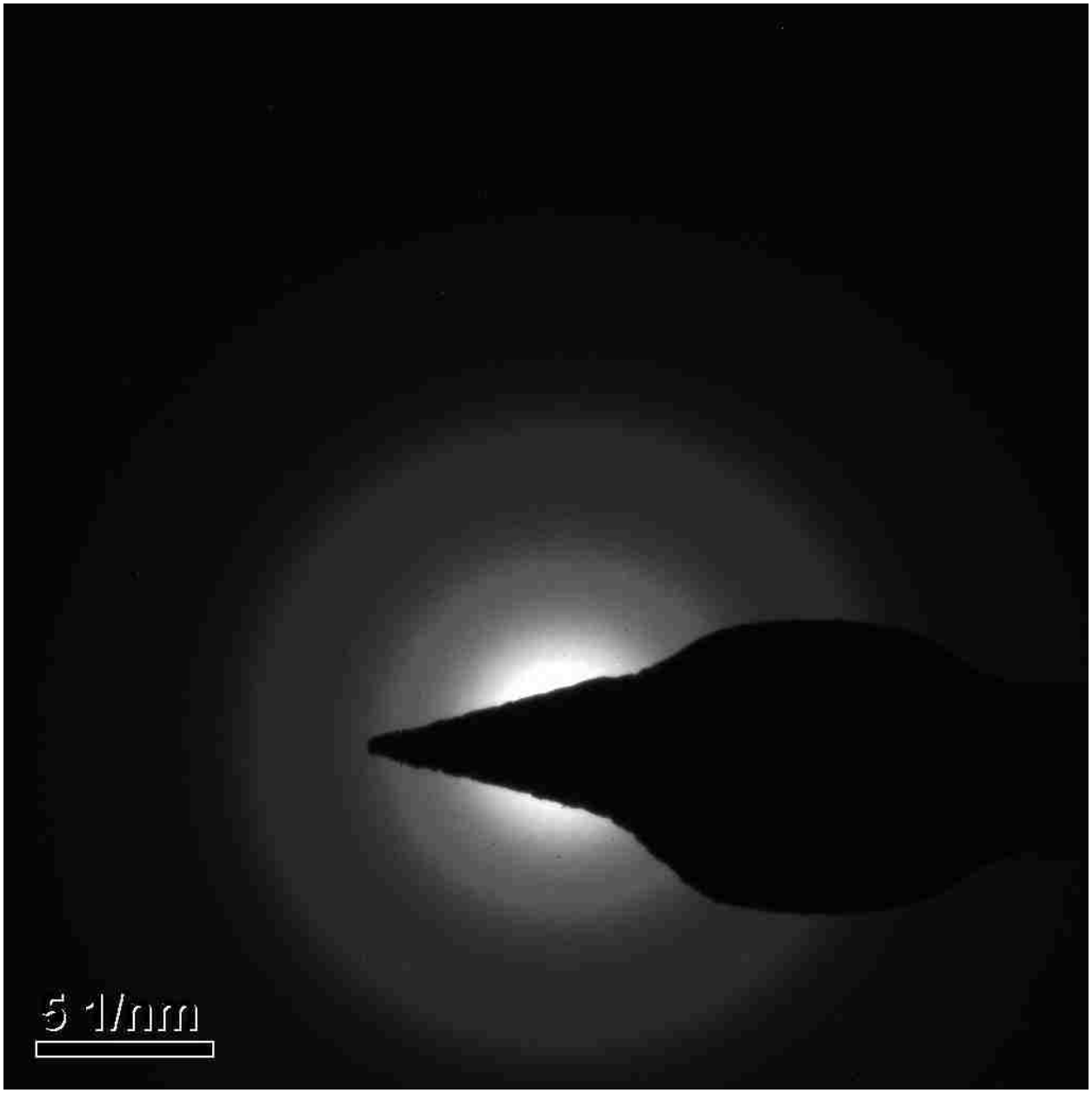

Figure 7: Selected area electron diffraction (SAED) image during HR-TEM of CuSiNG 4 showing amorphous nature of the silica matrix.

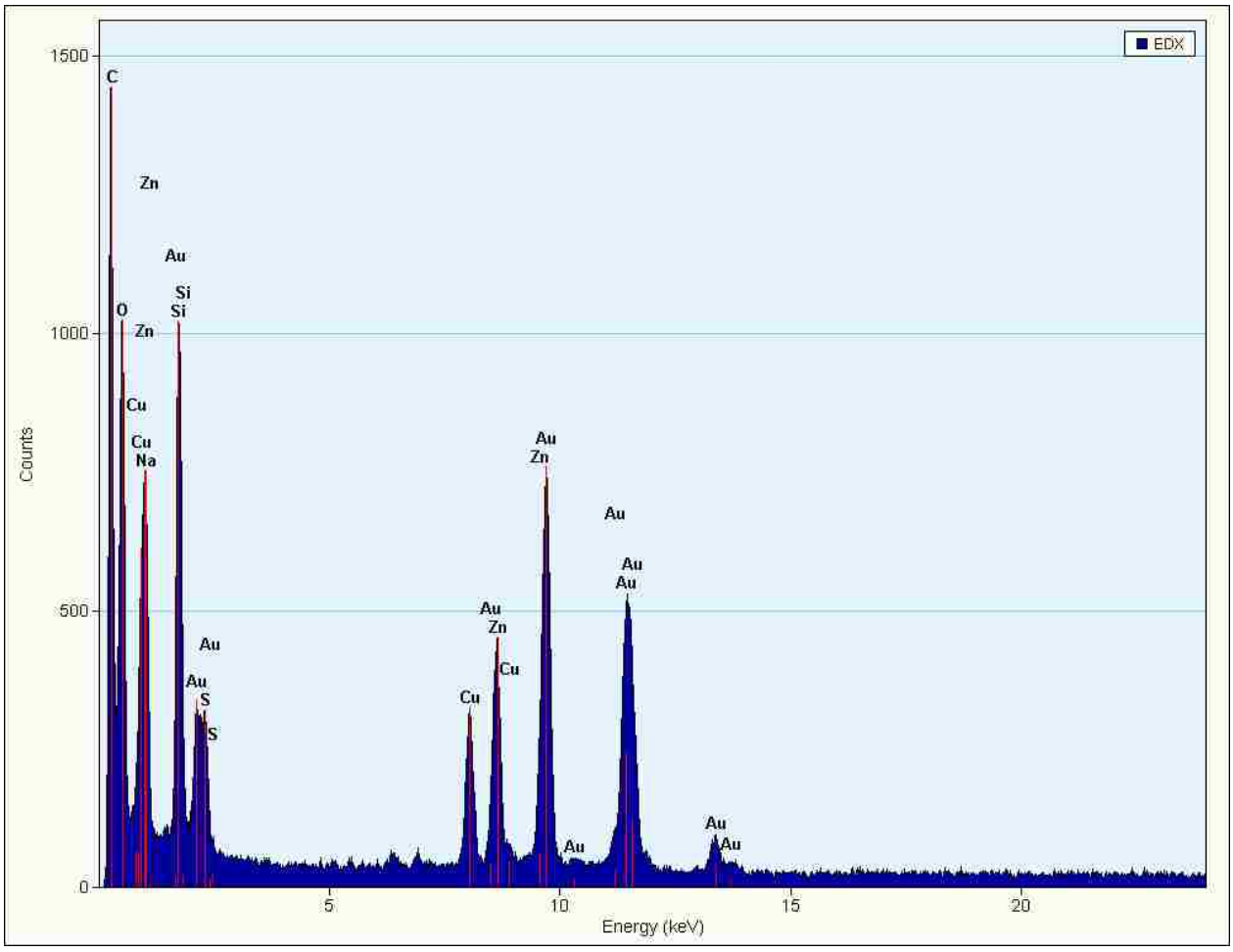

Figure 8: Energy-dispersive X-ray spectroscopy (EDX) for elemental analysis of CuSiNG B during HR-TEM

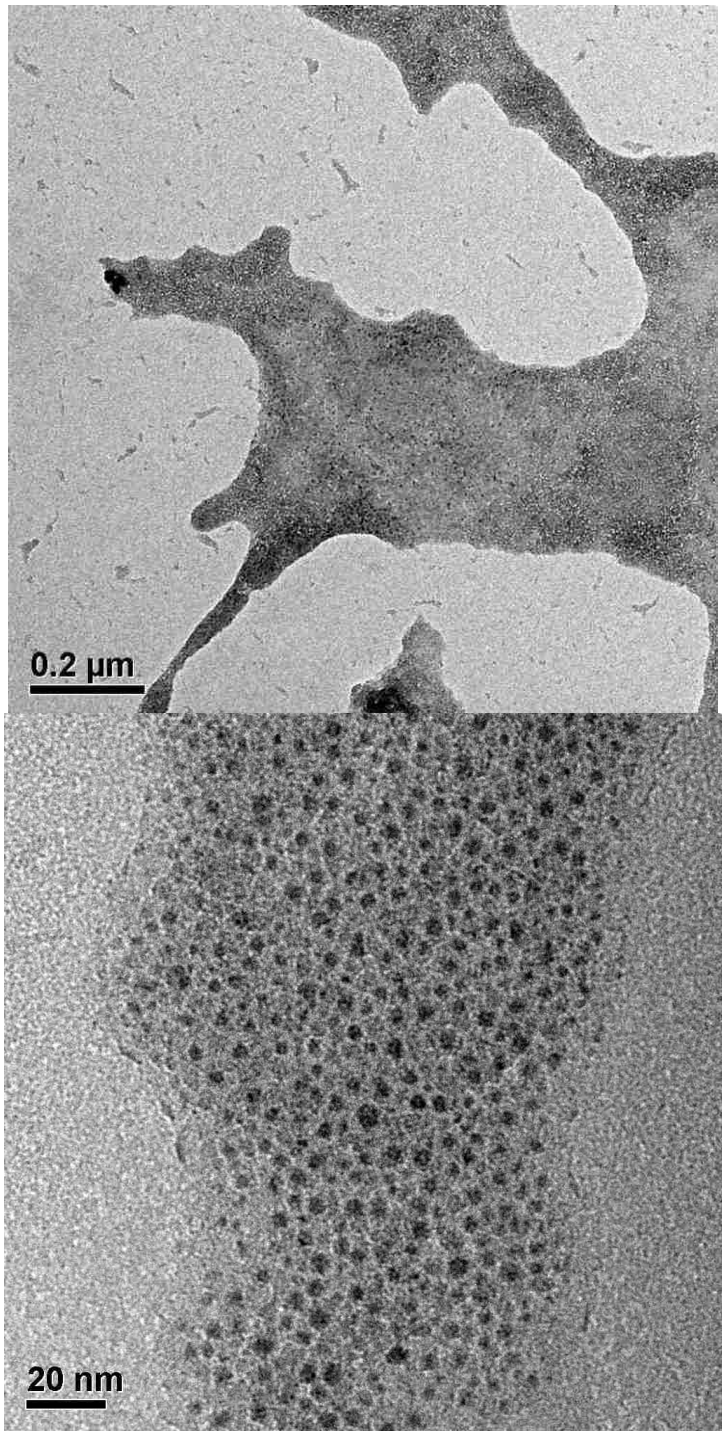

Figure 9: HR-TEM (low mag) images of CuSiNG B with scattered dark contrast confirming presence of electron-rich material.

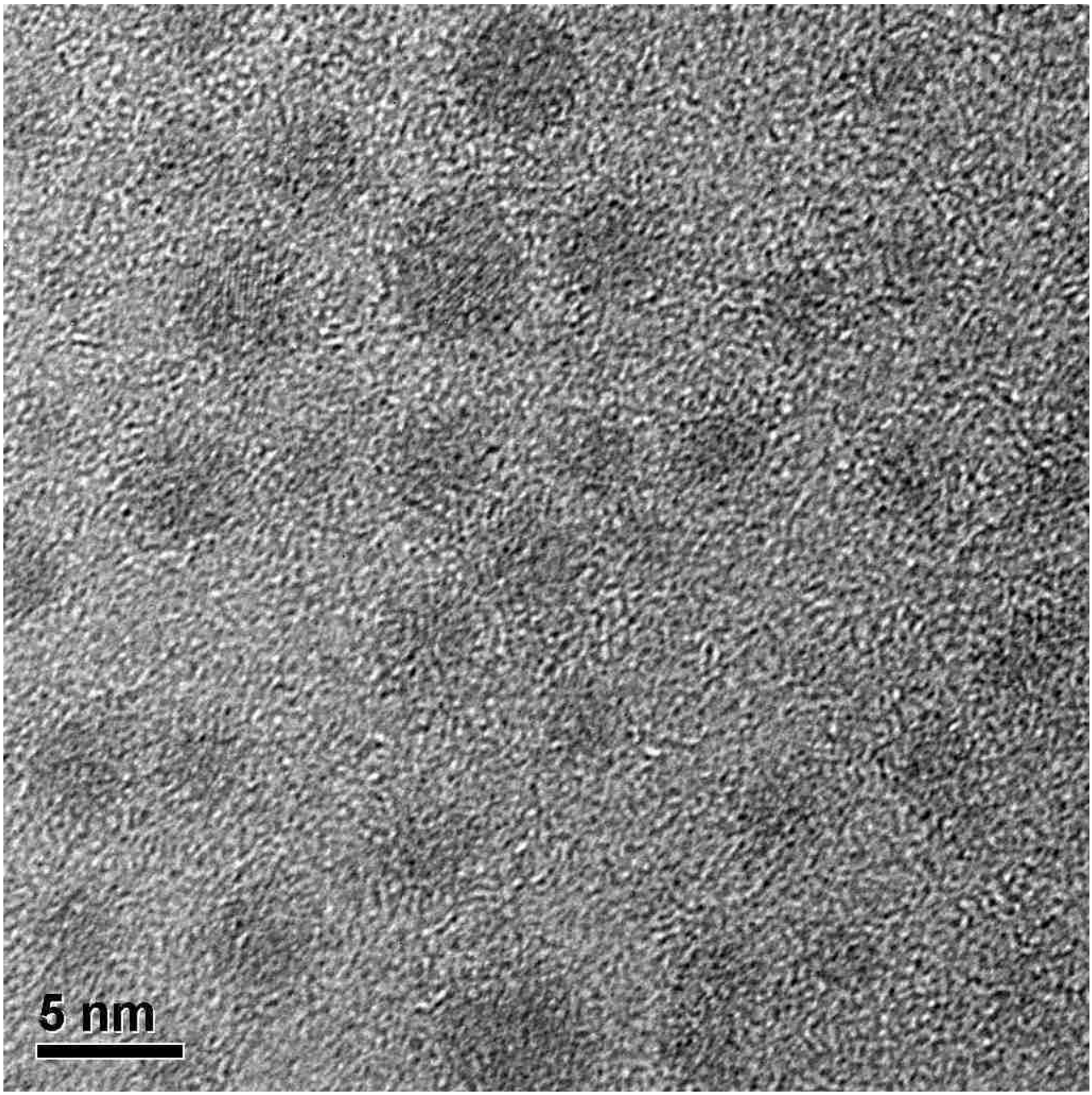

Figure 10: HR-TEM image of CuSiNG B with scattered dark contrast confirming presence of electron-rich material (circled in yellow). Lattice spacing measured from enlarged HR-TEM (Inset) is ~ 3.02 Å, ~2.52 Å and ~2.32 Å.

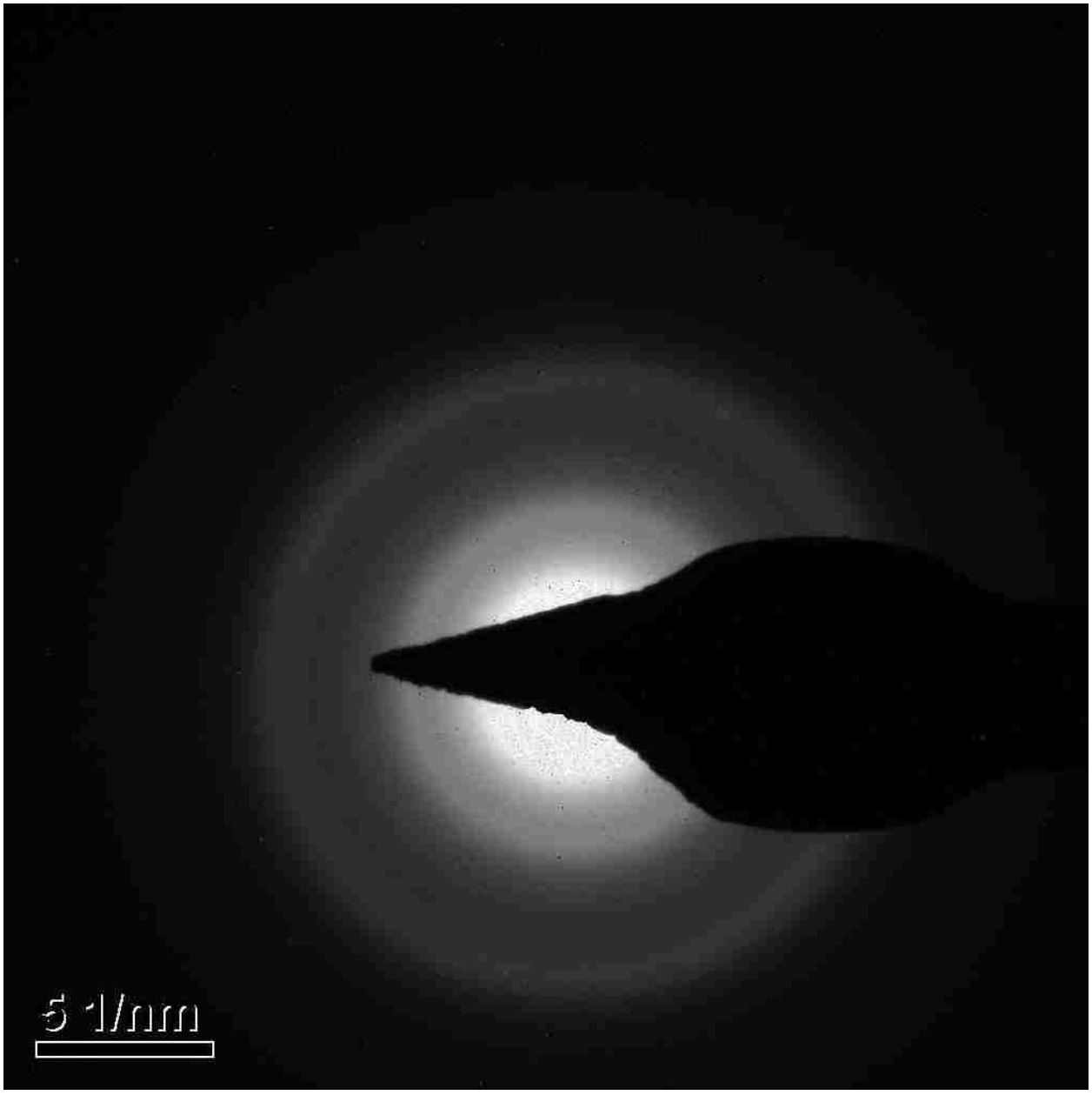

Figure 11: Selected area electron diffraction (SAED) image during HR-TEM of CuSiNG B showing amorphous nature of the silica matrix.

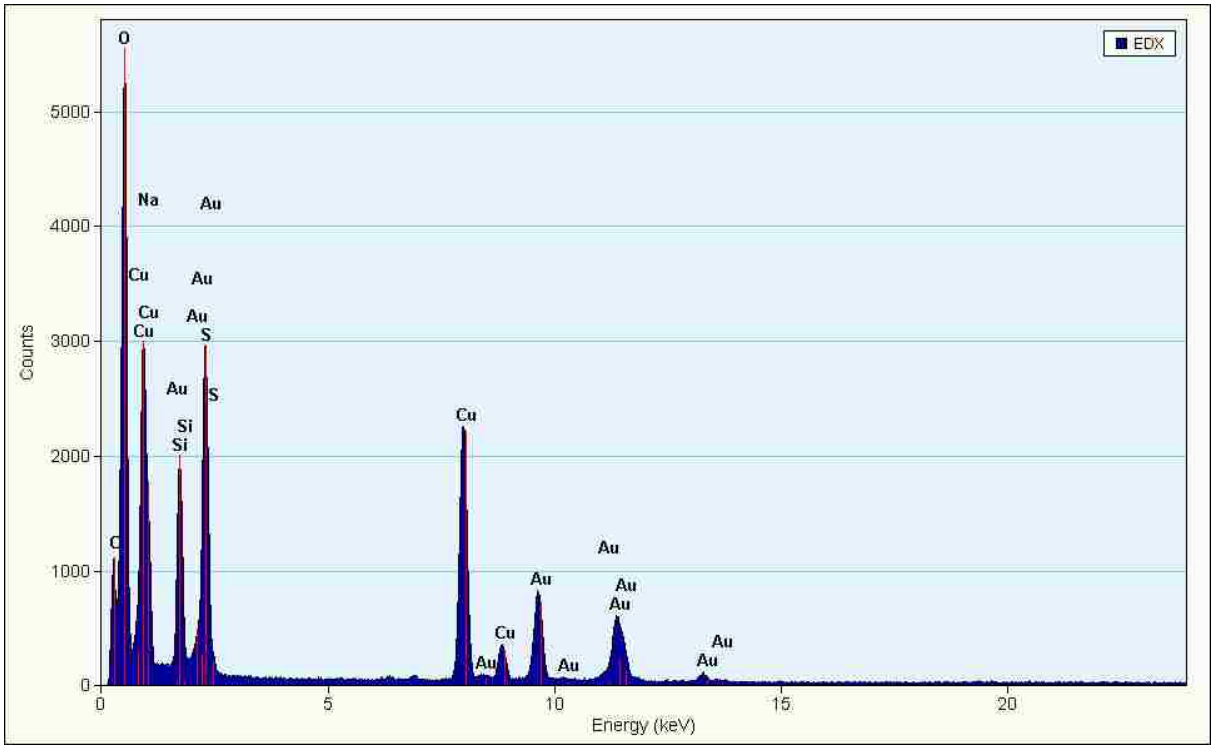

Figure 12: Energy-dispersive X-ray spectroscopy (EDX) for elemental analysis of CuSiNG S during HR-TEM.

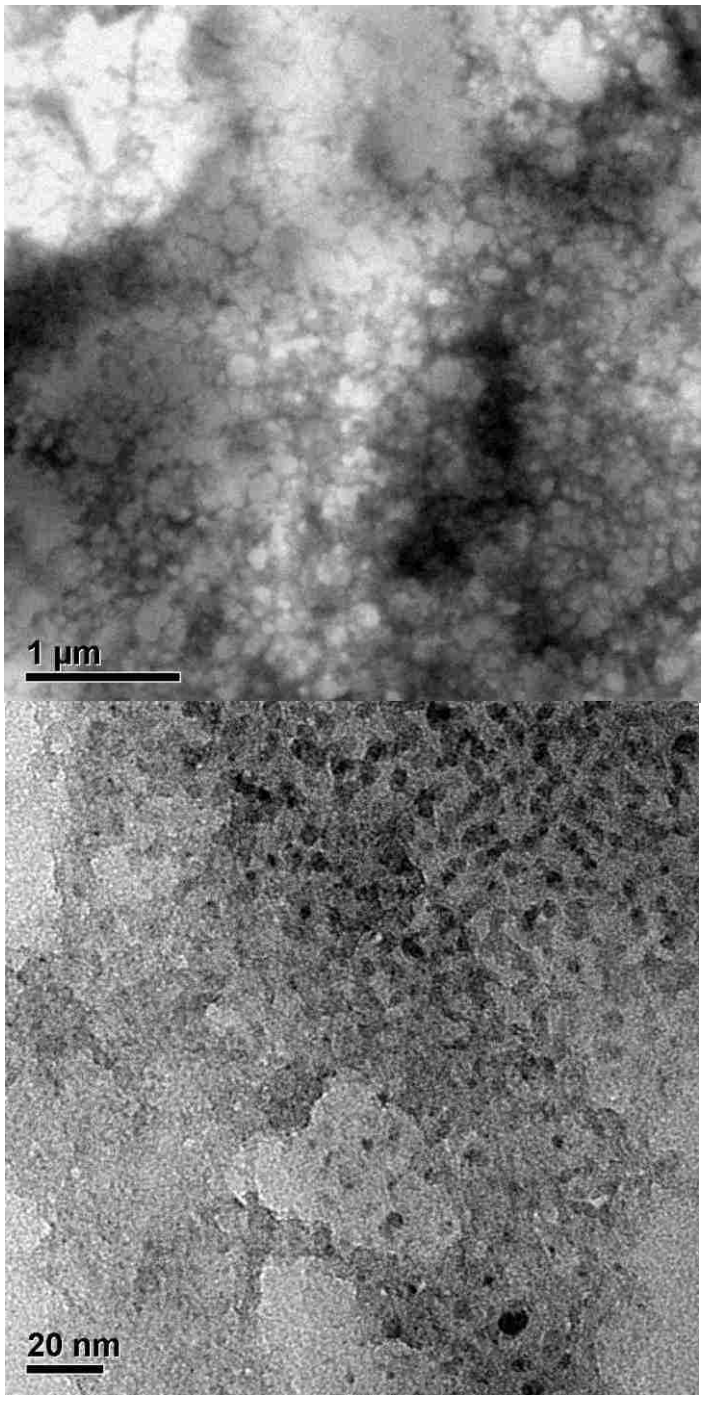

Figure 13: HR-TEM (low mag) image of CuSiNG S with scattered dark contrast confirming presence of electron-rich material.

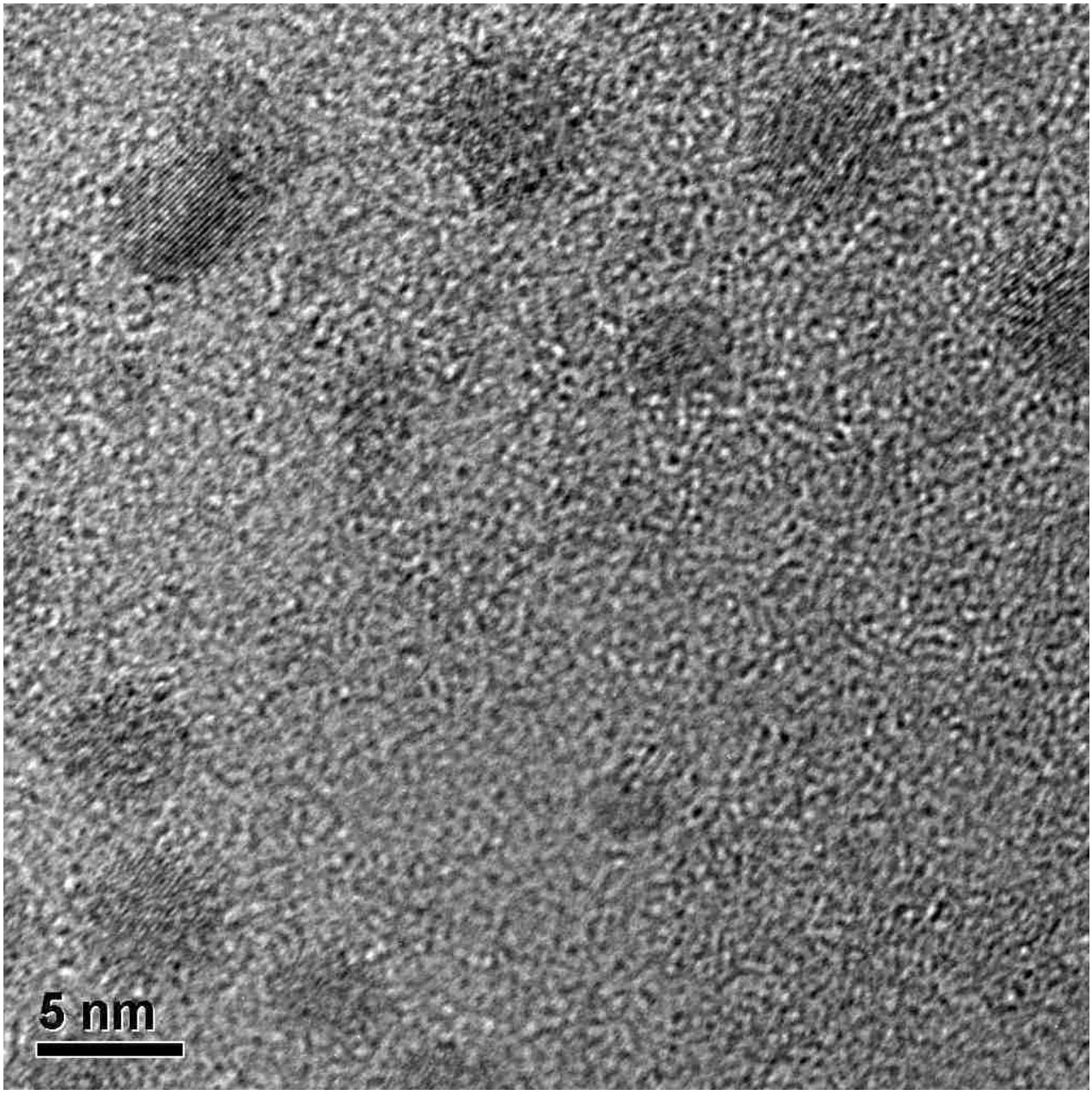

Figure 14: HR-TEM image of CuSiNG S with scattered dark contrast confirming presence of electron-rich material (circled in yellow). Lattice spacing measured from enlarged HR-TEM (Inset) is ~ 2.09 Å, ~ 2.32 Å, 3.02 Å and ~2.47 Å.

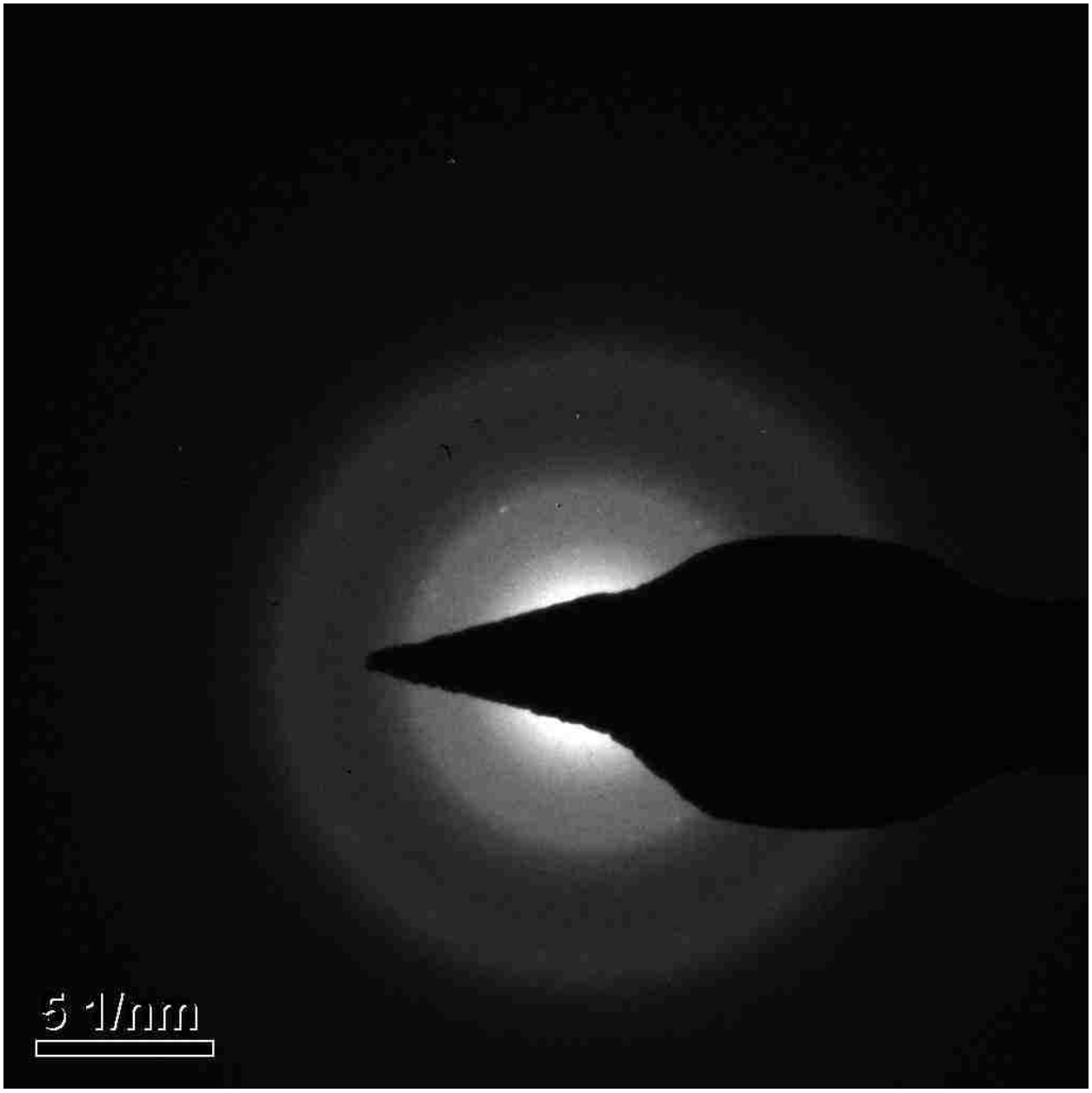

Figure 15: Selected area electron diffraction (SAED) image during HR-TEM of CuSiNG S showing amorphous nature of the silica matrix.

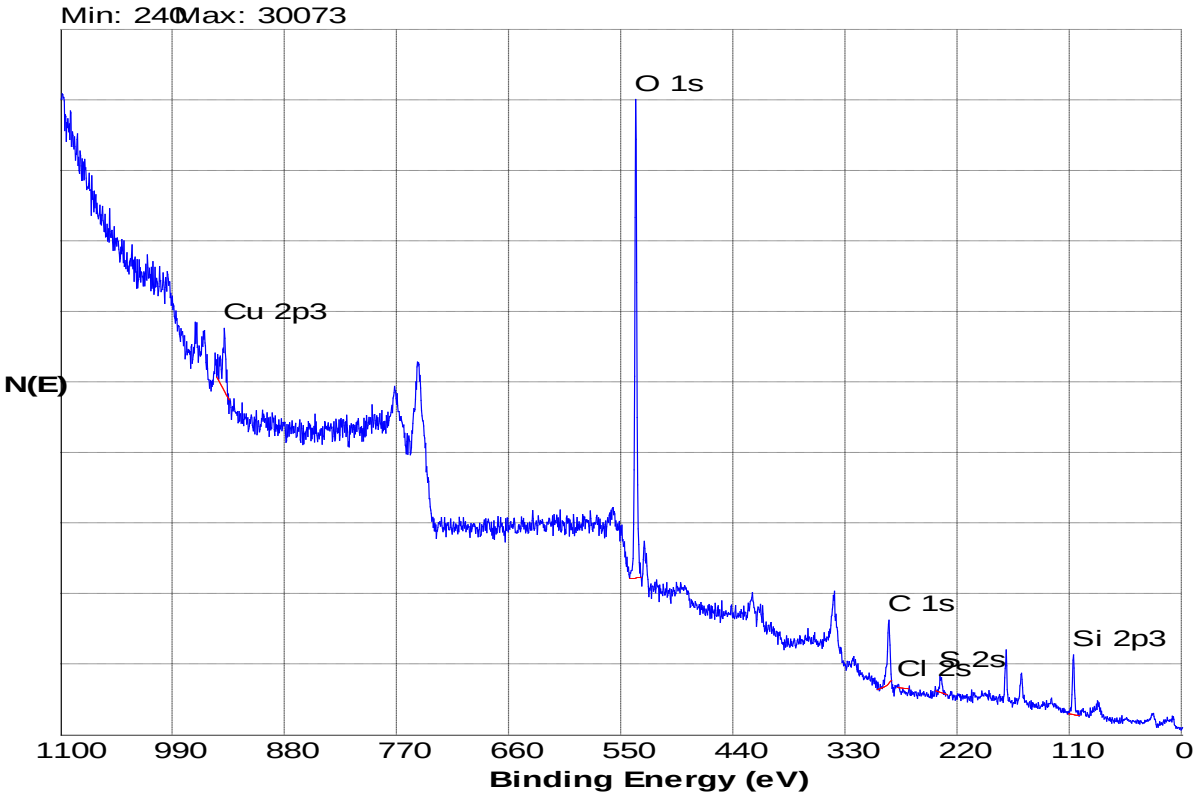

Figure 16: X-ray photoelectron spectroscopy (XPS) survey spectra of CuSiNG 4 showing the elemental composition.

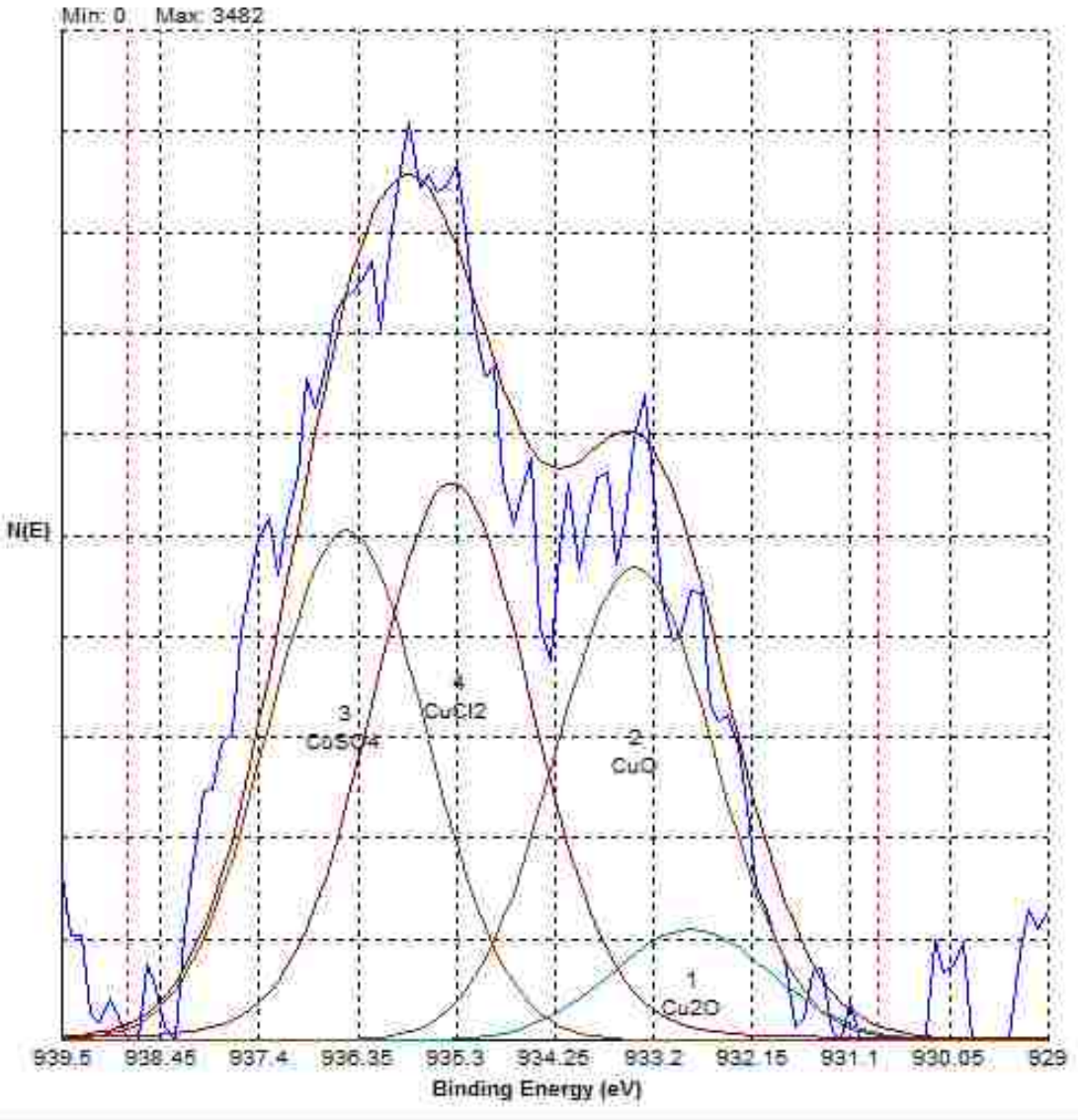

Figure 17: X-ray photoelectron spectroscopy (XPS) high-resolution spectra of Cu in CuSiNG 4.

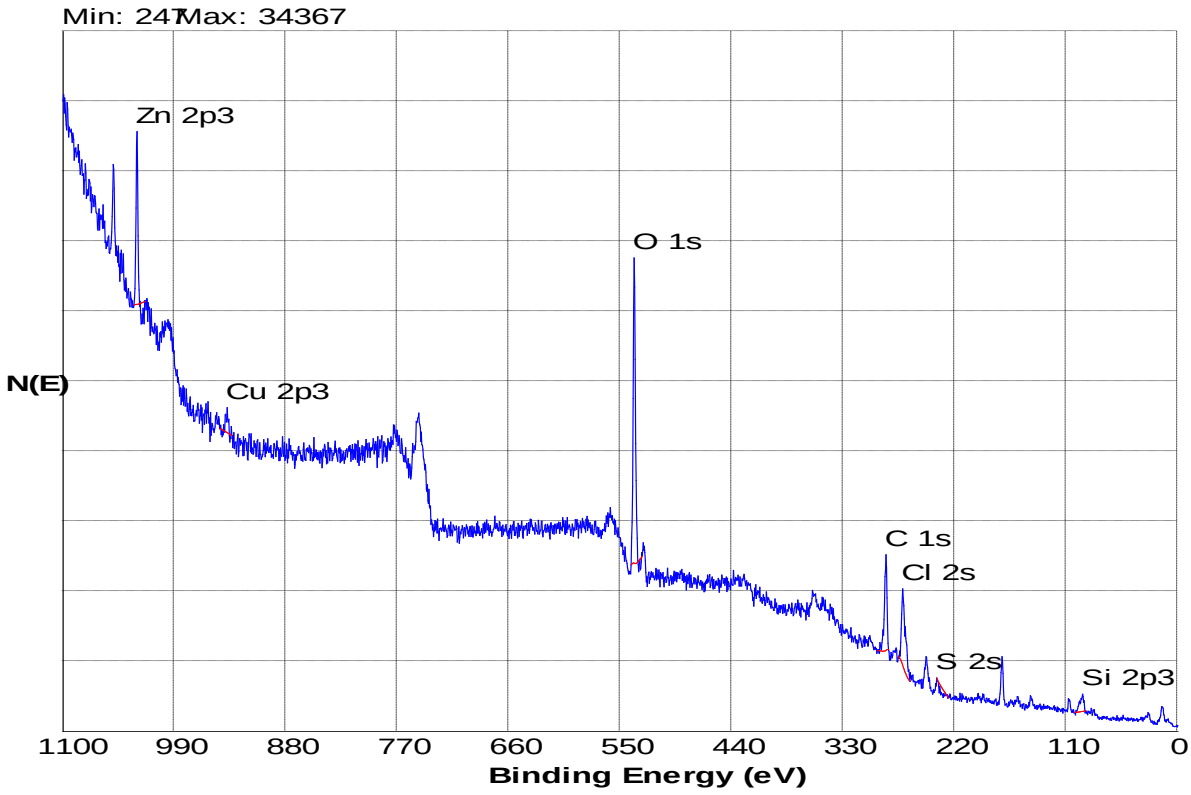

Figure 18: X-ray photoelectron spectroscopy (XPS) survey spectra of CuSiNG B showing the elemental composition.

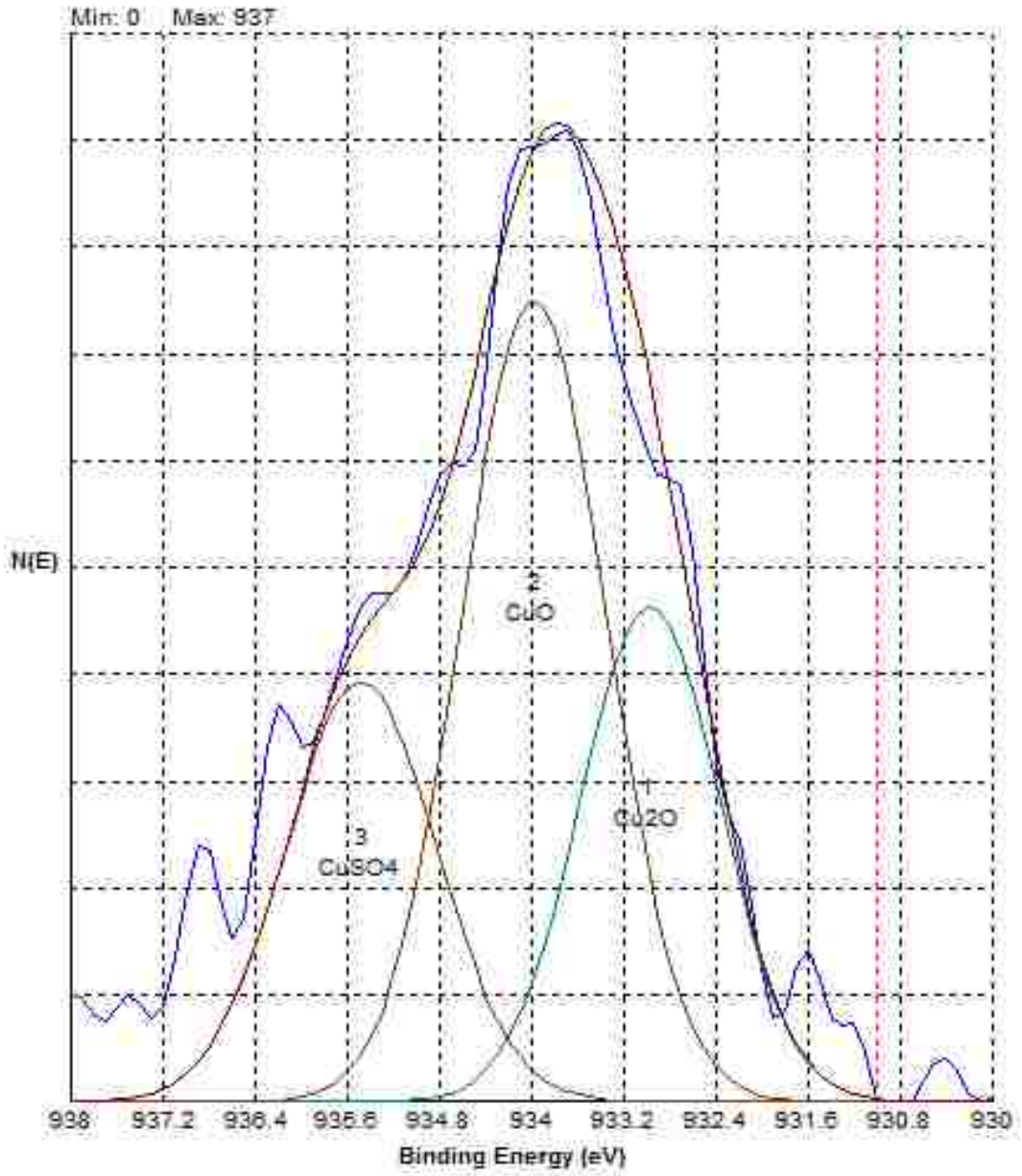

Figure 19: X-ray photoelectron spectroscopy (XPS) high-resolution spectra of Cu in CuSiNG B.

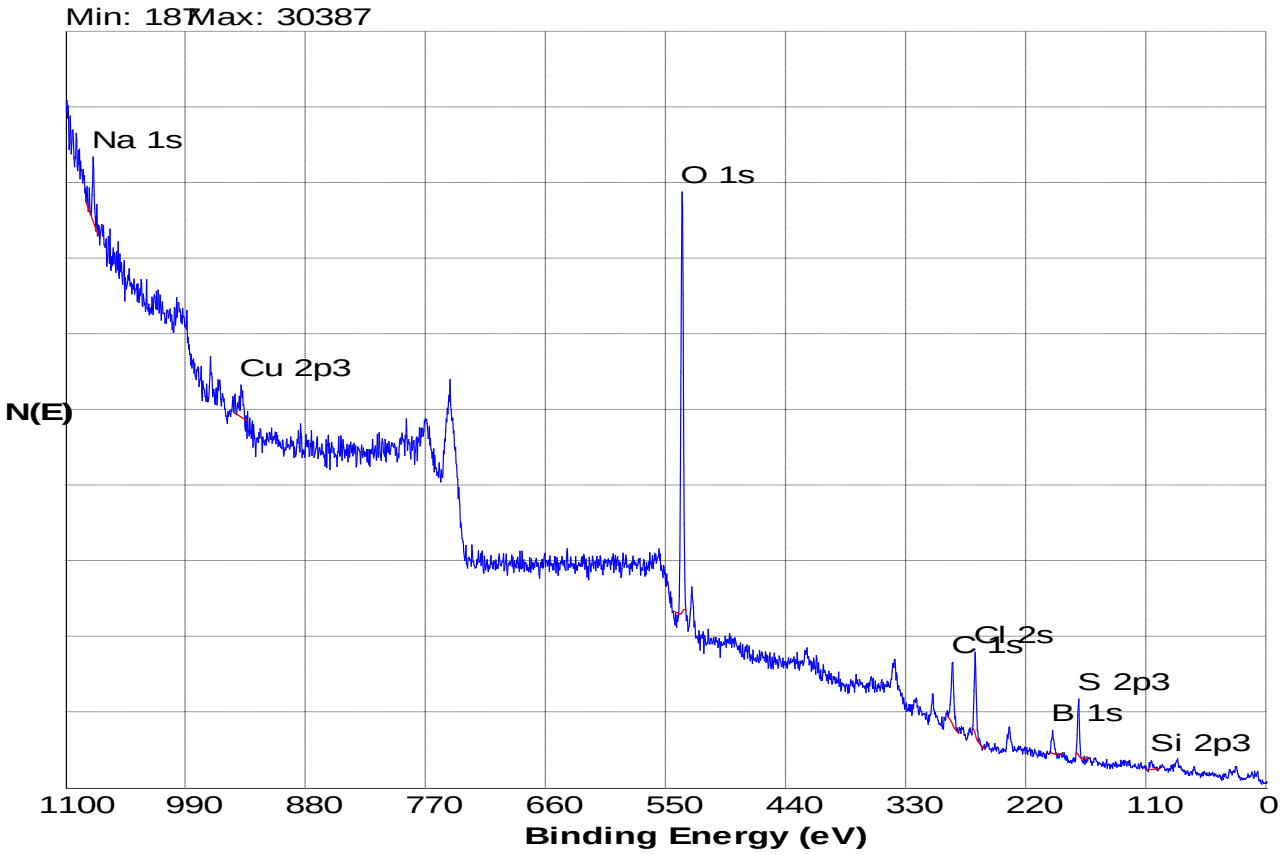

Figure 20: X-ray photoelectron spectroscopy (XPS) survey spectra of CuSiNG S showing the elemental composition.

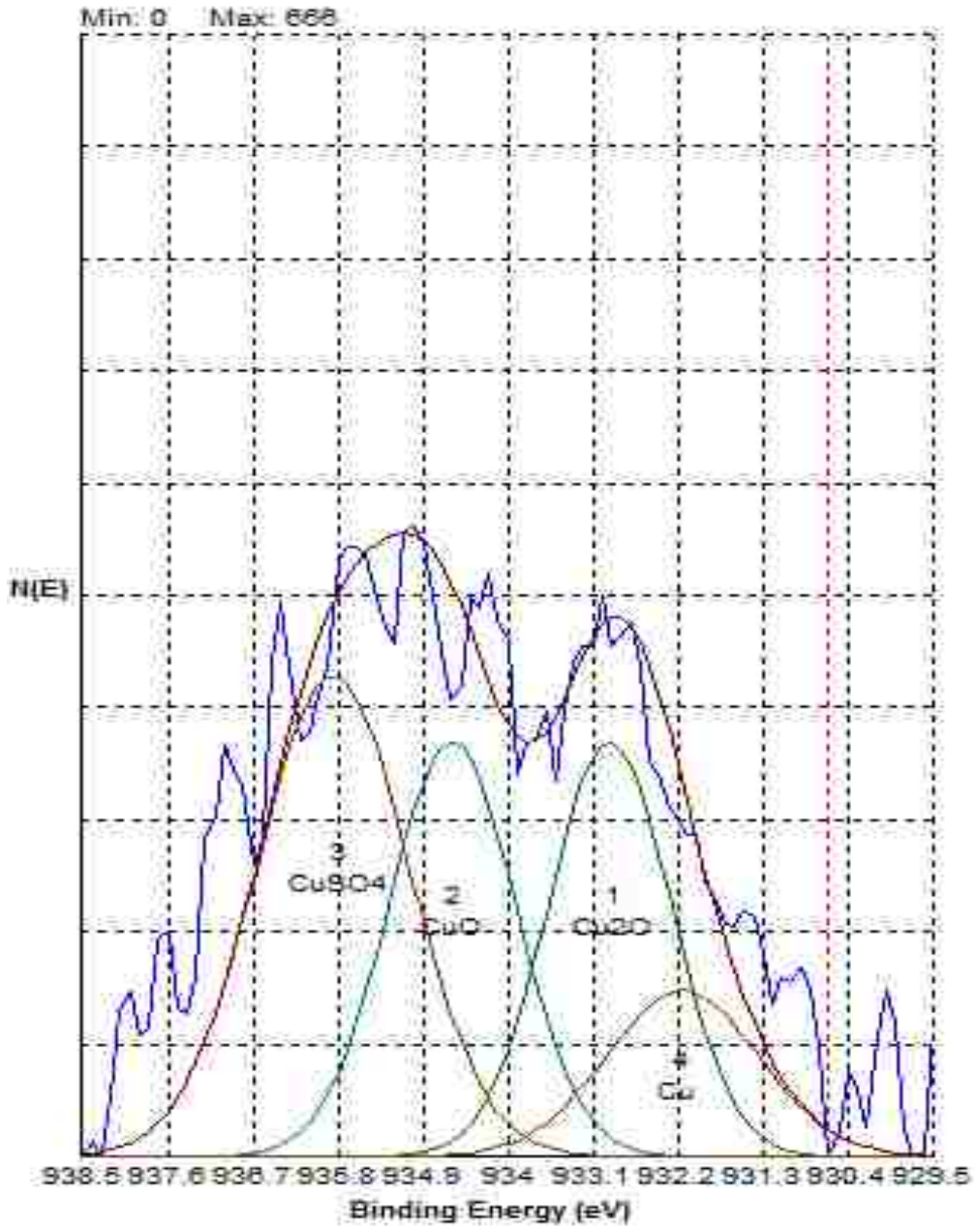

Figure 21: X-ray photoelectron spectroscopy (XPS) high-resolution spectra of Cu in CuSiNG S.

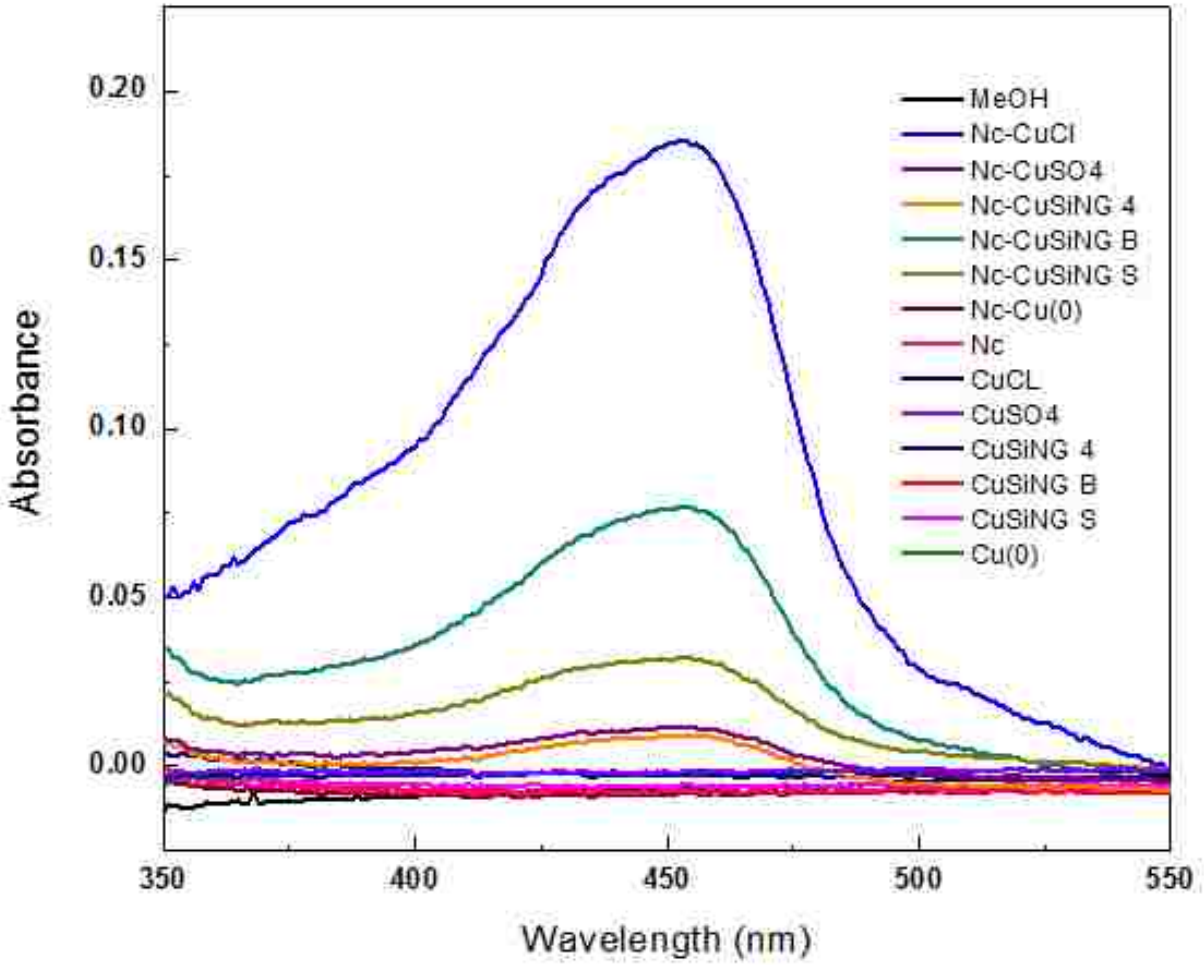

Figure 22: UV-Vis spectra of CuSiNG materials chelated with Neocuproine (Nc).

Cu(I)-Neocuproine complex absorbance peak seen at ~455nm.

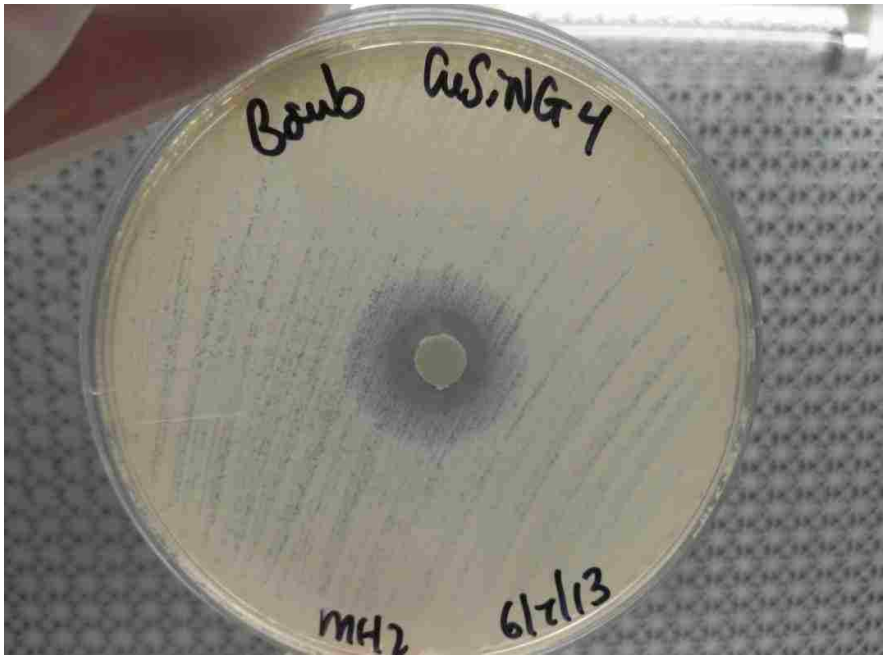

Figure 23- Clear zone of inhibition of ~ 18mm by CuSiNG 4 against *B.subtilis*

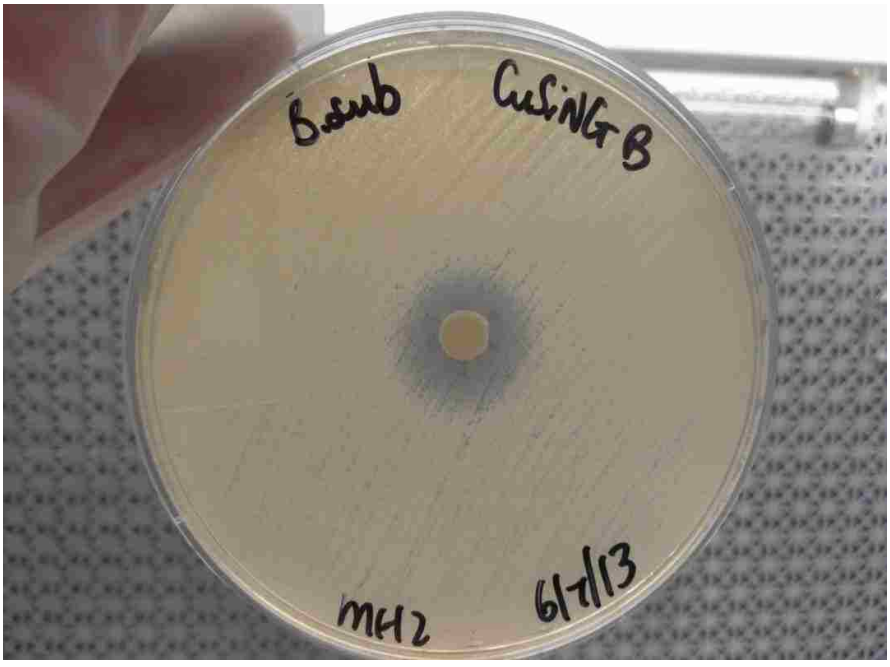

Figure 24- Clear zone of inhibition of ~ 17mm by CuSiNG B against *B.subtilis*

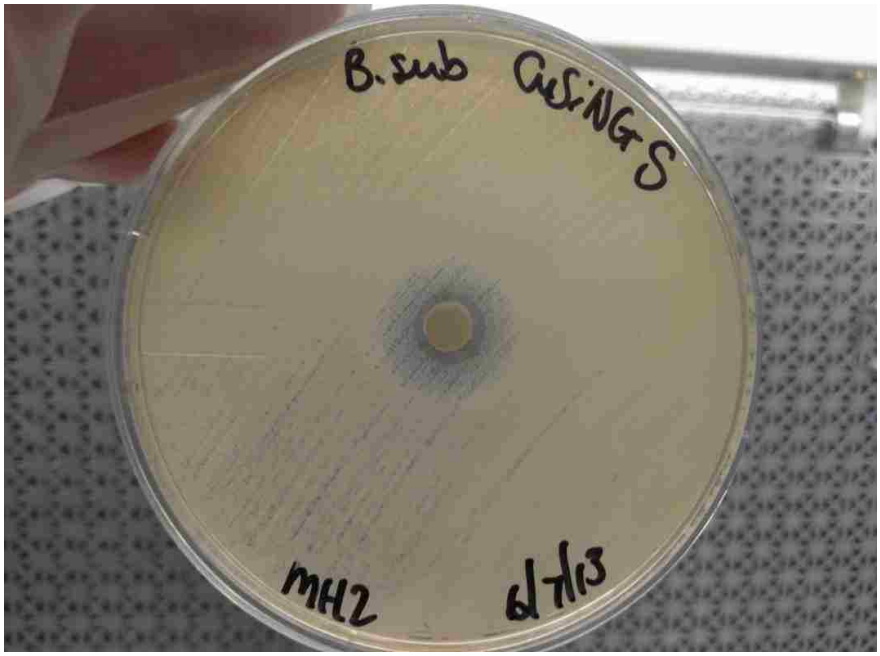

Figure 25- Clear zone of inhibition of ~ 16mm by CuSiNG S against *B.subtilis*

Table 1: Zone of Inhibition of Cu materials against *X.alfalfae*, *B.subtilis* and *E.coli* (mm).

Material	**Zone of Inhibition (mm)**					
	X.alfalfae		***B.subtilis***		***E.coli***	
	Avg.	**σ**	**Avg.**	**σ**	**Avg.**	**σ**
CuSiNG 4	**17.7**	**0.94**	**18.3**	**2.18**	**12**	**1.41**
CuSiNG B	**17.3**	**1.7**	**19**	**1.41**	**12.7**	**0.94**
CuSiNG S	**16.7**	**1.89**	**18.3**	**1.7**	**11.7**	**1.44**
$CuSO_4$	**16.3**	**2.05**	**16.7**	**1.7**	**10.3**	**1.25**
CuCl	**16.3**	**1.63**	**16**	**1.41**	**10.7**	**0.46**
Kocide	**13.3**	**3.3**	**9.7**	**1.7**	**7.3**	**0.47**
SiNG	**0**	**0**	**0**	**0**	**0**	**0**

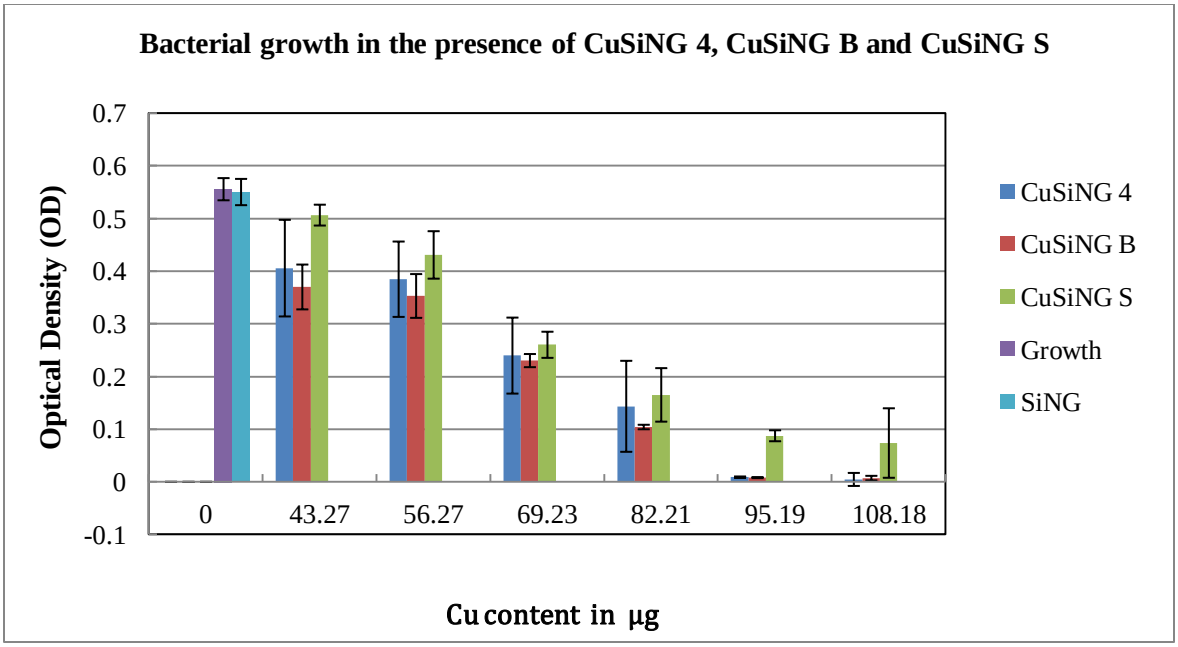

Figure 26: Histogram of growth inhibition of *X.alfalfae* by CuSiNG 4, CuSiNG B and CuSiNG S

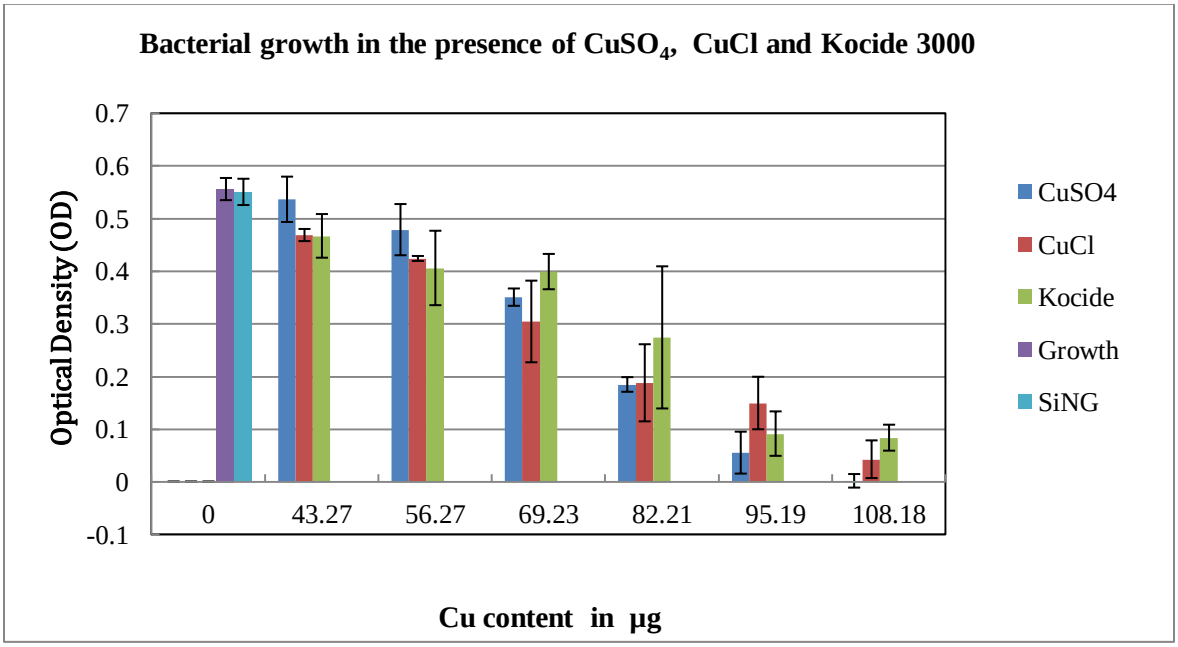

Figure 27: Histogram of growth inhibition of *X.alfalfae* by CuSO4, CuCl and Kocide 3000.

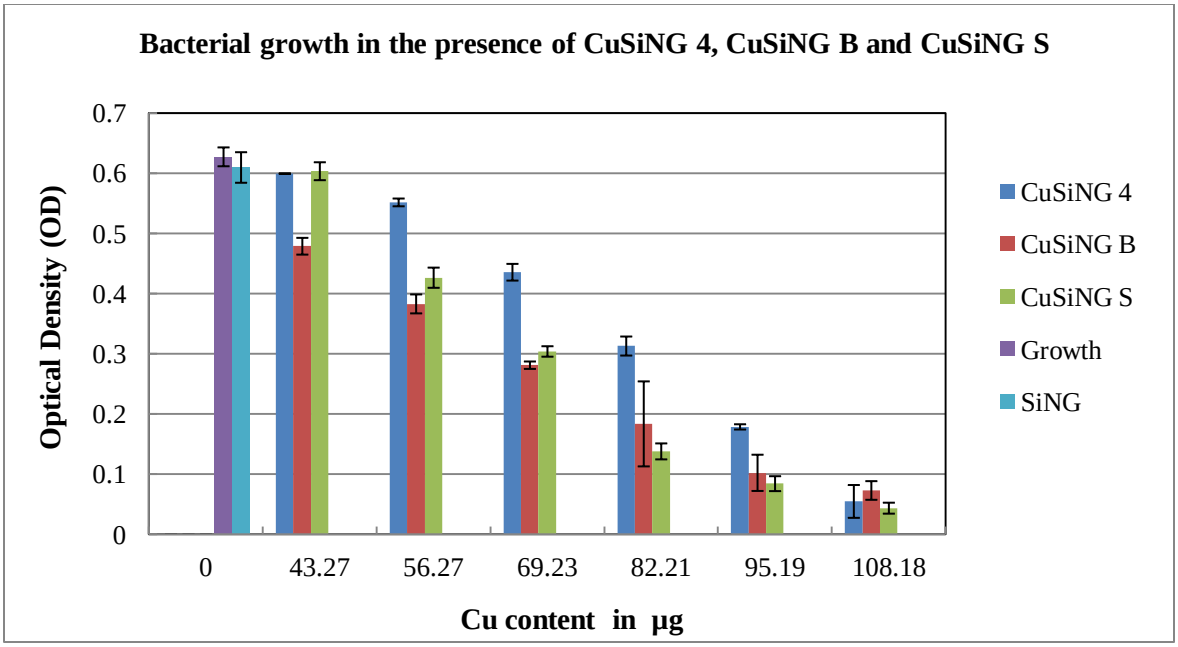

Figure 28: Histogram of growth inhibition of *B.subtilis* by CuSiNG 4, CuSiNG B and CuSiNG S

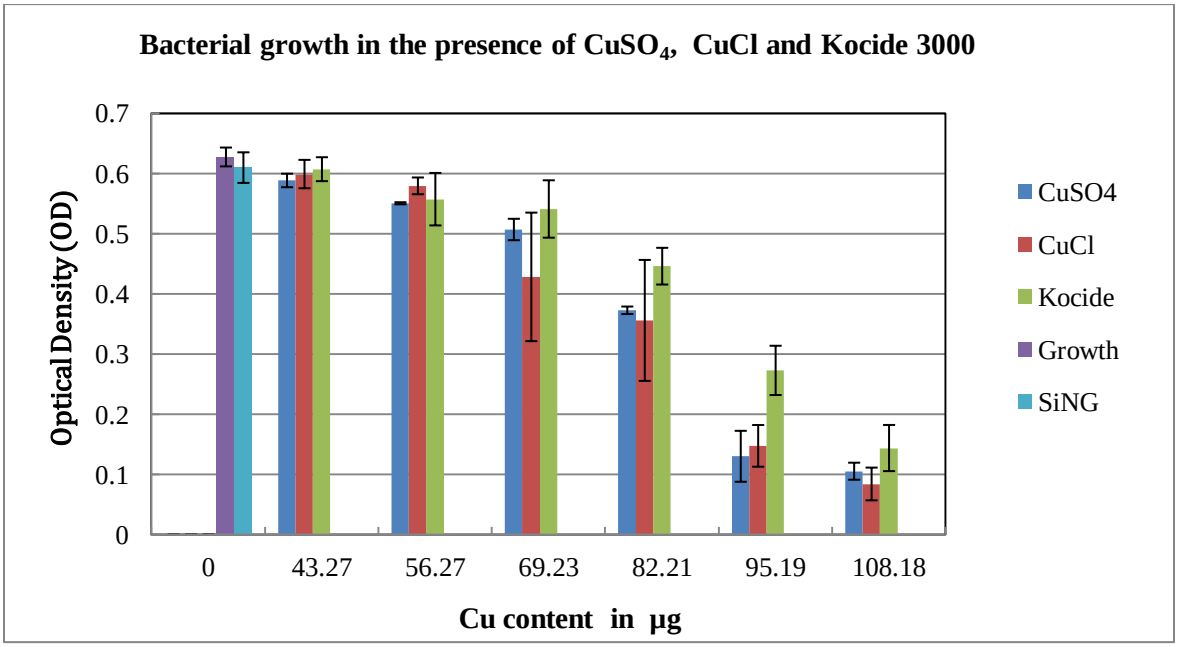

Figure 29: Histogram of growth inhibition of *B.subtilis* by CuSO4, CuCl and Kocide 3000

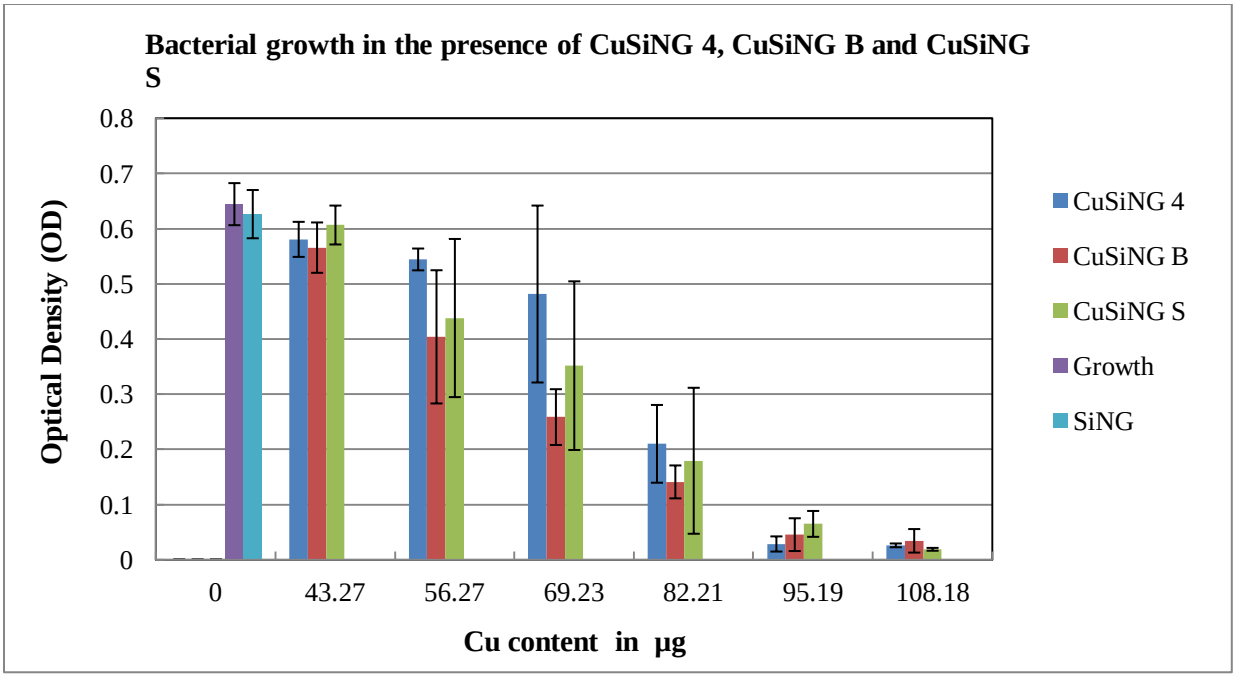

Figure 30: Histogram of growth inhibition of *E.coli* by CuSiNG 4, CuSiNG B and CuSiNG S

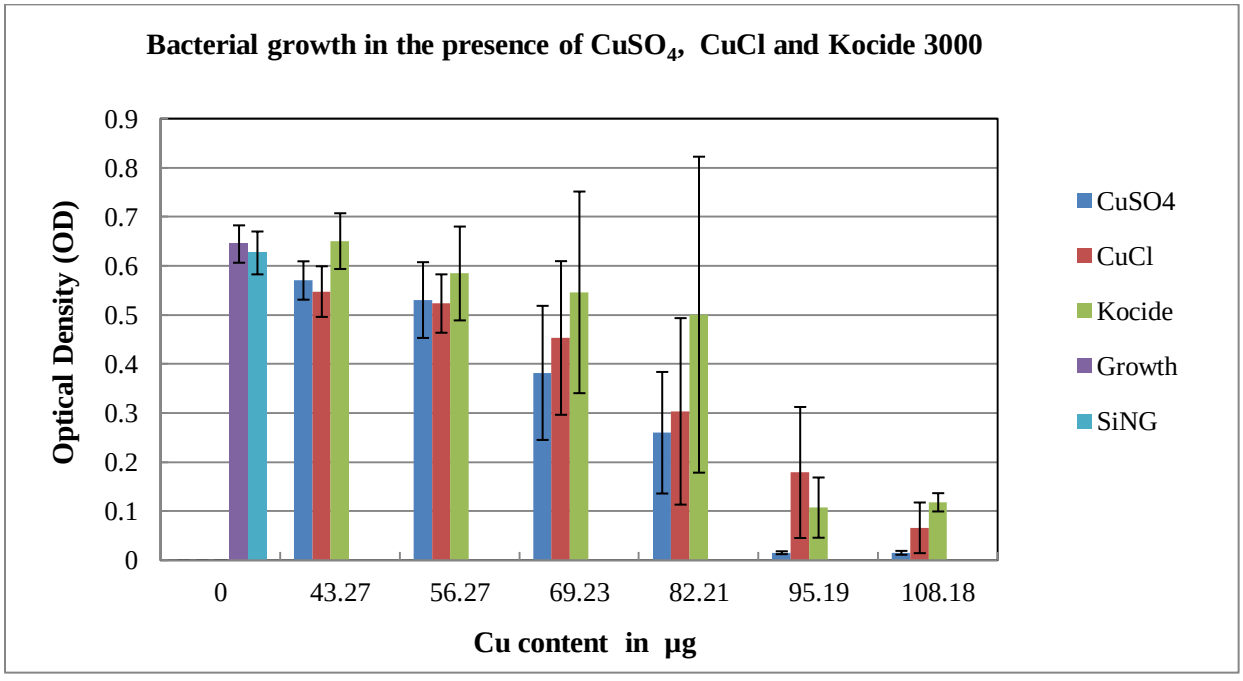

Figure 31: Histogram of growth inhibition of *E.coli* by CuSO4, CuCl and Kocide 3000.

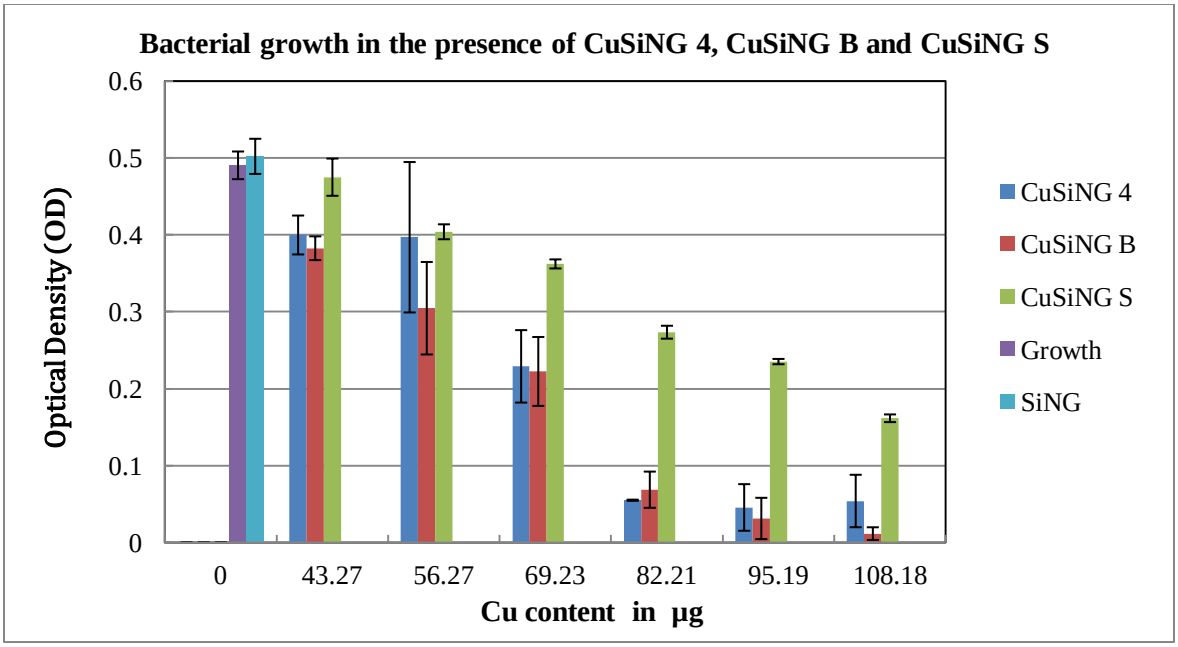

Figure 32: Histogram of growth inhibition of *E.coliΔcopA1(del)* by CuSiNG 4, CuSiNG B and CuSiNG S

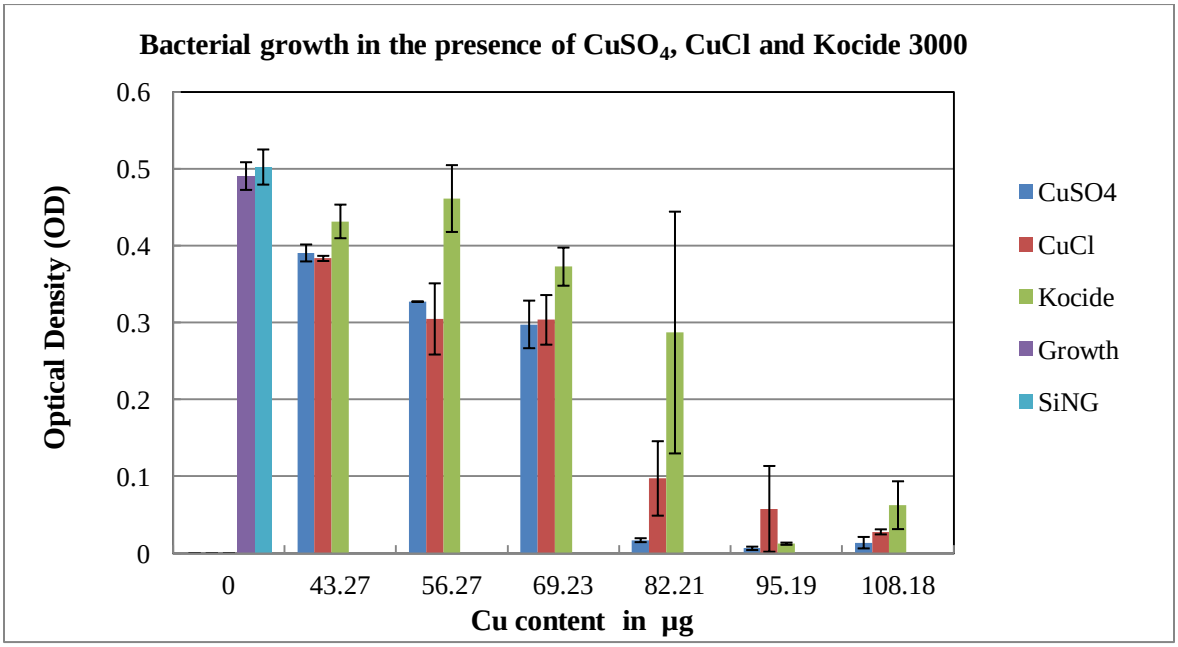

Figure 33: Histogram of growth inhibition of *E.coliΔcopA1(del)* by CuSO4, CuCl and Kocide 3000.

Table 2: MIC of Cu materials against *X.alfalfae, B.subtilis, E.coli and E.coliΔcopA1(del)* in µg/ mL(ppm) Cu.

	Minimum Inhibitory Concentration (MIC) (µg/ mL(ppm) Cu)			
	X.alfalfae	***B.subtilis***	***E.coli***	***E.coli ΔcopA1(del)***
CuSiNG 4	**5.4**	**5.4**	**5.4**	**5.4**
CuSiNG B	**2.7**	**2.7**	**2.7**	**1.35**
CuSiNG S	**2.7**	**2.7**	**5.4**	**2.7**
$CuSO_4$	**10.8**	**5.4**	**10.8**	**5.4**
CuCl	**2.7**	**2.7**	**5.4**	**2.7**
Kocide	**10.8**	**10.8**	**10.8**	**10.8**

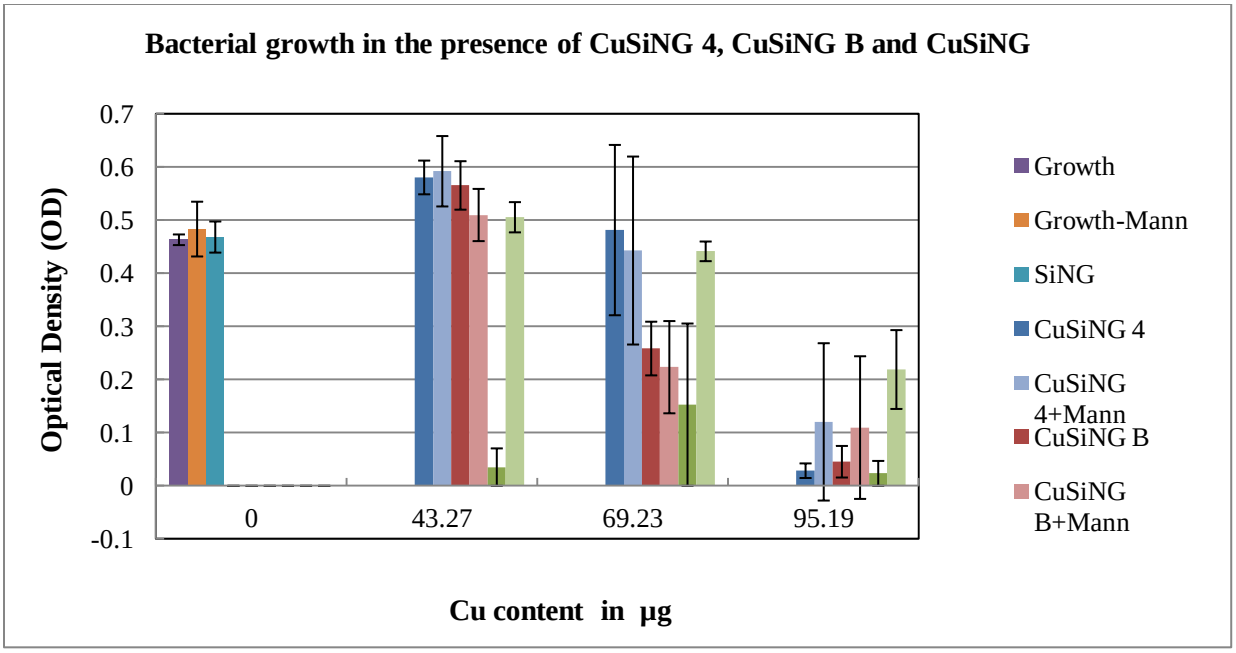

Figure 34: Histogram of growth inhibition of *E.coli* by CuSiNG 4, CuSiNG B and CuSiNG S in the presence and absence of D-Mannitol

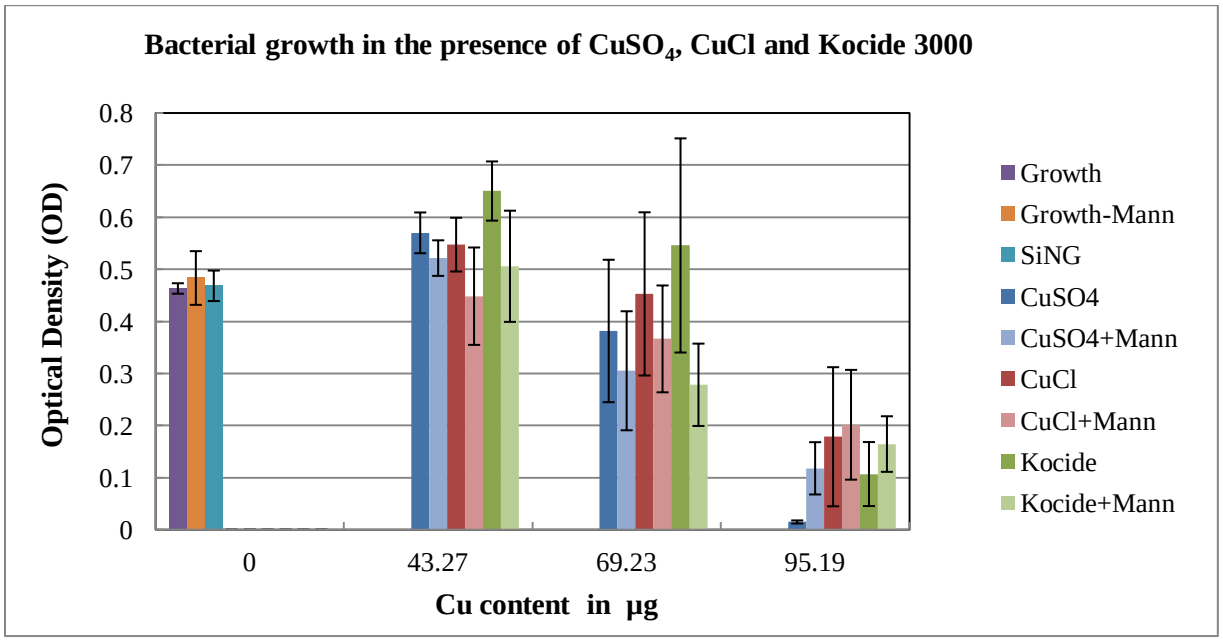

Figure 35: Histogram of growth inhibition of *E.coli* by CuSO4, CuCl and Kocide 3000 in the presence and absence of D-Mannitol

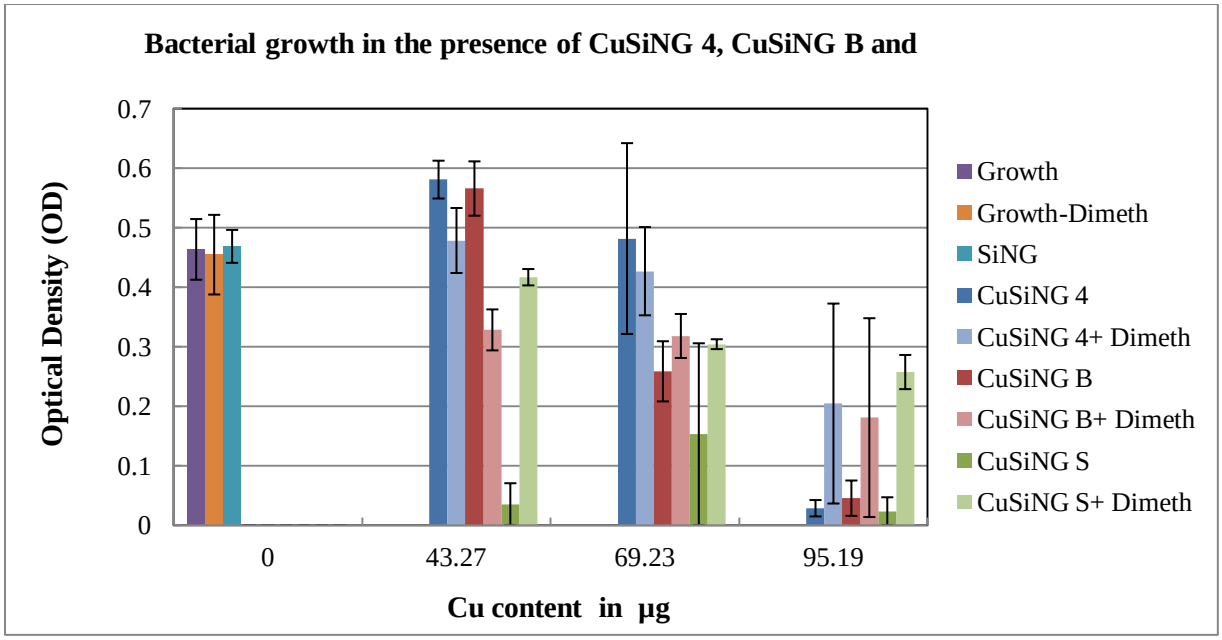

Figure 36: Histogram of growth inhibition of *E.coli* by CuSiNG 4, CuSiNG B and CuSiNG S in the presence and absence of Dimethylthiourea

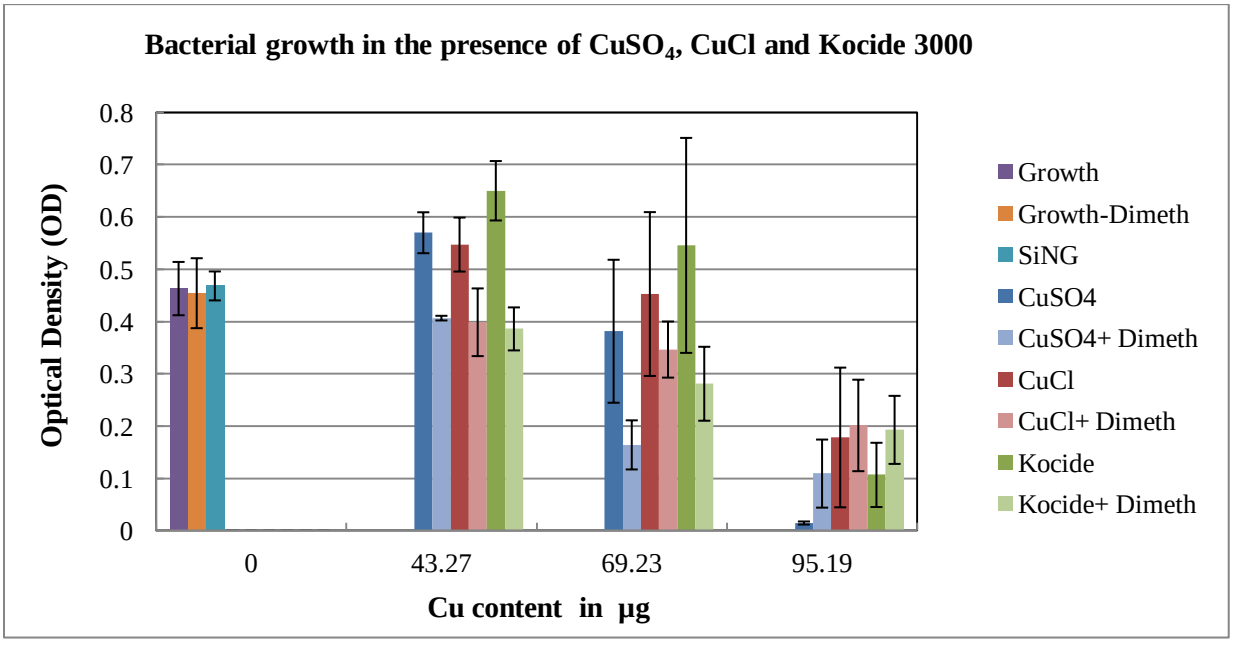

Figure 37: Histogram of growth inhibition of *E.coli* by CuSO4, CuCl and Kocide in the presence and absence of Dimethylthiourea

Table 3: Phytotoxicity of Cu materials against Hamlin orange.

Tested Material	Metallic Cu Content (ppm)	Phytotoxicity Rating		
		24 hr	48 hr	72 hr
Untreated	NA	-	-	-
SiNG	NA	-	-	-
CuSiNG 4	90	-	-	-
	450	-	-	-
	900	-	-	-
CuSiNG B	90	-	-	-
	450	-	-	-
	900	-	-	-
CuSiNG S	90	-	-	-
	450	-	-	-
	900	-	-	-
CuCl	90	-	-	-
	450	-	-	-
	900	-	-	-
$CuSO_4$	90	-	-	-
	450	-	-	-
	900	-	-	-
Kocide 3000	90	-	-	-
	450	-	-	-
	900	-	-	-

Table 4: Phytotoxicity of Cu materials against Vinca sp.

Tested Material	Metallic Cu Content (ppm)	Phytotoxicity Rating		
		24 hr	48 hr	72 hr
Untreated	NA	-	-	-
SiNG	NA	-	-	-
CuSiNG 4	90	-	-	-
	450	-	+	+
	900	+	++	++
CuSiNG B	90	-	-	-
	450	-	+	+
	900	+	++	++
CuSiNG S	90	-	-	-
	450	-	+	+
	900	+	++	++
CuCl	90	-	-	-
	450	-	-	-
	900	-	+	+
$CuSO_4$	90	-	-	-
	450	+	+	+
	900	+	++	++
Kocide 3000	90	-	-	-
	450	-	-	-
	900	-	-	-

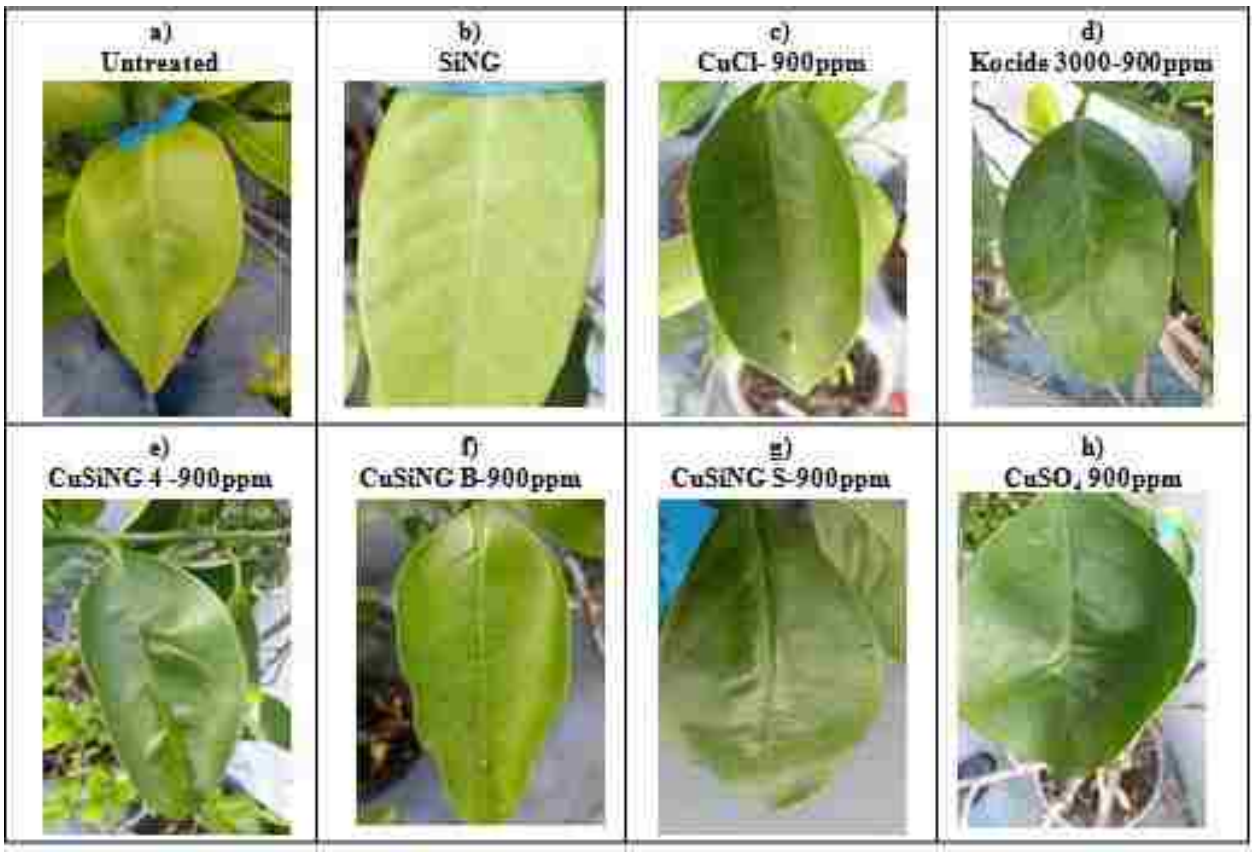

Figure 38: Cu materials applied on *Hamlin orange* at 900 ppm metallic Cu content.

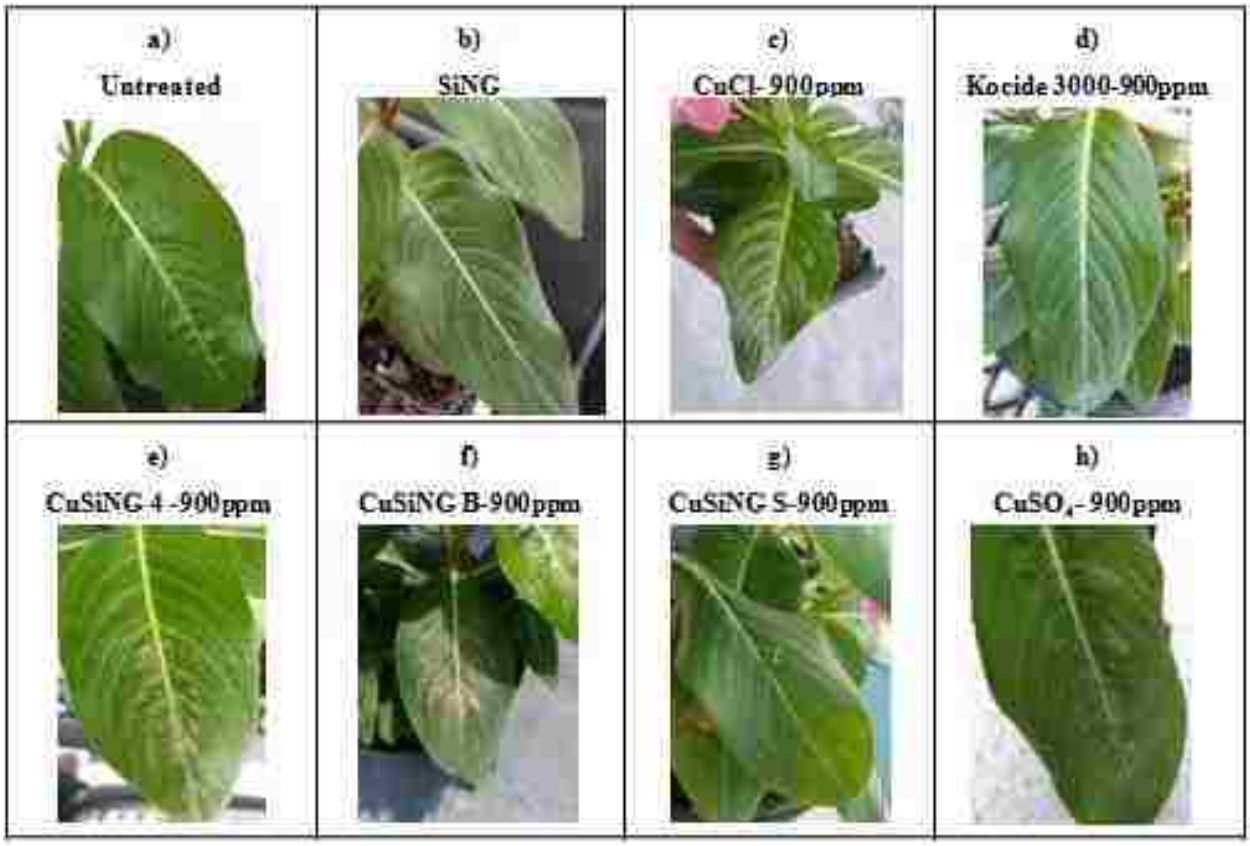

Figure 39: Cu materials applied on *Vinca sp*. at 900 ppm metallic Cu content.

CHAPTER 4- CONCLUSION

Copper loaded silica nanogel (CuSiNG 4) was successfully synthesized using an acid hydrolysis protocol [34]. Because the reaction does not require further purification, copper loading into the silica matrix is very substantial, as confirmed by AAS measurements. To create a Cu mixed valence system, CuSiNG 4 was subsequently reduced in two separate ways using different reducing agents (Zinc and Sodium borohydride) to create CuSiNG B and CuSiNG S. All CuSiNG materials were stable, transparent and blue in color.

HR-TEM revealed a nicely dispersed silica matrix with high numbers of Cu crystallites, indicating high Cu loading. Crystallites within the matrix varied in size, leading to the confirmation that they were all not the same type of Cu compound. Further HR-TEM observations revealed a variety of Cu crystallites types within CuSiNG materials. CuSiNG 4 was found to contain mostly CuO crystallites with minimal Cu_2O crystallites. CuSiNG B possessed CuO crystallites with a higher proportion of Cu_2O crystallites than CuSiNG 4. CuSiNG S was found to contain crystallites for CuO, Cu_2O and metallic Cu. The different Cu valence states identified in HR-TEM were further confirmed by XPS data. The states identified in XPS were $CuSO_4$, $CuCl_2$, CuO, Cu_2O and Cu. Cu (I) content was further observed by use of the Cu (I) specific chelator, neocuproine. The UV-Vis spectra of the Cu (I)-neocuproine showed that CuSiNG 4 had minimal Cu (I) while CuSiNG B and CuSiNG S possessed increased amounts of Cu (I). The increase in Cu (I) from CuSiNG 4 to CuSiNG B and CuSiNG S confirms that a Cu mixed valence system was successfully created.

Antimicrobial efficacy of CuSiNG materials were found to be higher than the Cu controls $CuSO_4$ and Kocide 3000. CuCl exhibited strong antimicrobial efficacy but is unsuitable for

formula due to its low soluble. Solubilizing CuCl would require extremely low pHs which correlate to high levels of plant tissue damage. Attempts to create a copper loaded silica nanogel with CuCl as the Cu source were not successful. CuSiNG B and CuSiNG S exhibited a further enhanced antimicrobial properties as compared to CuSiNG 4, indicating that a Cu mixed valence system is more efficient at compromising bacterial cell viability than a Cu(II) only system. CuSiNG B was created using zinc powder which may influence its antimicrobial efficacy but CuSiNG S was created using sodium borohydride. Therefore the increased efficacy of CuSiNG S can only be attributed to the increased Cu (I) content.

The hydroxyl radical scavengers D-Mannitol and N, N-dimethylthiourea were used to indirectly confirm the presence of hydroxyl radicals and observe their action in bacterial cell death. In presence of the scavengers, *E.coli* was able to survive or resist Cu toxicity to a certain extent. Higher bacterial survival confirms that hydroxyl radicals play a role in the mechanism of Cu toxicity.

Phytotoxicity testing was used to evaluate the safety levels at which Cu materials can be used to protect plants from potential pathogens. All materials tested were found to be safe on the model citrus species used, *Hamlin orange,* while higher concentrations were toxic on the ornamental species *Vinca sp*. Kocide 3000 showed no toxicity on *Vinca sp* but its antimicrobial efficacy is much lower than CuSiNG materials. While CuSiNG materials exhibited toxicity at higher concentrations, their antimicrobial efficacy indicates that they can be applied at lower rates while providing adequate protection. Kocide 3000 protects at higher rates, thereby leading to larder amounts of Cu accumulation within the environment.

CuSiNG materials were synthesized and proven to be more efficient than control materials. Increasing the Cu (I) content of CuSiNG showed better efficacy, allowing for reducing Cu amounts while maintaining protection. Further research into the specific mechanisms of Cu toxicity can lead to further improvements in protection formulation and even the development of alternative sources to Cu formulas.

REFERENCES

1. **Borkow, J.G.a.G.,** ***Copper as a Biocidal Tool.*** **Current Medicinal Chemistry, 2005. 12(18): p. 2163-2175.**
2. **J.Gabbay, G.B.a.,** ***Putting copper into action:copper-impregnated products with potent biocidal activities.*** **The FASEB Journal, 2004. 18(14): p. 1728-1730.**
3. **S.L Warnes, S.M.G., H.T. Michels and C.W. Keevil,** ***Biocidal Efficacy of Copper Alloys against Pathogenic Enterococci Involves Degradation of Genomic and Plasmid DNAs.*** **Applied and Environmental Microbiology, 2010. 76(16): p. 5390-5401.**
4. **Amit Singh, V.K., Alexander Angerhofer,Bao Do,Gavin MacDonald and Brij Moudgil,** ***Copper Coated Silica Nanoparticles for Odor Removal.*** **Langmuir, 2010. 26(20): p. 15837-15844.**
5. **Kelechi.C.Anyaogu, A.V.F.a.D.C.N.,** ***Synthesis, Characterization and Antifouling Potential of Functionalized Copper Nanoparticles.*** **Langmuir, 2008. 24: p. 4340-4346.**
6. **S. L. Warnes, V.C.a.C.W.K.,** ***Mechanism of copper surface toxicity in Escherichia coli O157:H7 and Salmonella involves immediate membrane depolarization followed by slower rate of DNA destruction which differs from that observed for Gram-positive bacteria.*** **Environmental Microbiology, 2012. 14(7): p. 1730–1743.**
7. **Thomas.J.Webster, J.T.S.a.,** ***Antimicrobial applications of nanotechnology:methods and literature.*** **International Journal of Nanomedicine, 2012(7): p. 2767-2781.**
8. **Phillips, D.R.L.a.D.H.,** ***Oxidative DNA damage mediated by copper(II), iron(II) and nickel(II) Fenton reactions: evidence for site-specific mechanisms in the formation of double-strand***

breaks, 8-hydroxydeoguanosine and putative intrastrand cross-links. **Mutation Research, 1999. 424: p. 23-36.**

9. **Imlay, J.A., *Pathways of Oxidative Damage.* Annu.Rev.Microbial, 2003. 57: p. 395-418.**

10. **Carin Thomas, M.M.M., Amy A. Diaz, David P. Cox, *Hydroxyl radical is produced via the Fenton reaction in submitochondrial particles under oxidative stress: implications for diseases associated with iron accumulation.* Redox Report, 2009. 14(3): p. 102-108.**

11. **Christophe Santo, N.T., Dietrich H.Nies and Gregor Grass, *Contribution of Copper Ion Resistance to Survival of Escherichia coli on Metallic Copper Surfaces.* Applied and Environmental Microbiology, 2008. 74(4): p. 977-986.**

12. **Okezie.I.Aruoma, B.H., Ewa.Gajewski and Miral Dizdaroglu, *Copper-ion dependent damage to the bases in DNA in the presence of hydrogen peroxide.* Journal of Biochemistry, 1991. 273: p. 601-604.**

13. **James.P.Kehrer, *The haber-Weiss reaction and mechanisms of toxicity.* Toxicology, 2000. 149: p. 43-50.**

14. **Imlay, L.M.a.J.A., *The iron-sulfur clusters of dehydratases are primary intracellular targets of copper toxicity.* PNAS, 2009. 106(20): p. 8344-8349.**

15. **Satish K. Singh, G.G., Christopher Rensing and William R. Montfort, *Cuprous Oxidase Activity of CueO from Escherichia coli.* Journal of Bacteriology, 2004. 186(22): p. 7815-7817.**

16. **Christopher Rensing, B.F., Rakesh Sharma, Bharati Mitra and Barry P.Rosen, *CopA: An Escherichia coli Cu(I)- Translocating P-type ATPase.* PNAS, 2000. 97(2): p. 652-656.**

17. **Sylvia Franke, G.G., Christopher Rensing and Dietrich H. Nies, *Molecular Analysis of the Copper-Transporting Efflux System CusCFBA of Escherichia coli.* Journal of Bacteriology, 2003. 185(13): p. 3804-3812.**

18. **Herzberg, D.H.N.a.M., *A fresh view of the cell biology of copper in enterobacteria.* Molecular Microbiology, 2012. 87(3): p. 447-454.**

19. **M.Pavlovic, *A review of Agribusiness Copper Use Effects on Environment.* Bulgarian Journal of Agricultural Science, 2011. 17(4): p. 491-500.**

20. **F.Behlau, J.B., A.Bergamin Filho,J.H.Graham, *Copper sprays and windbreaks for control of citrus canker on young orange tree in southern Brazil.* Crop Protection, 2008. 27: p. 807-813.**

21. **F.Behlau, J.B.J., J.H.Graham,R.P.Leite Jr, *Effect of frequency of copper applications on control of citrus canker and the yield of young bearing sweet orange trees.* Crop Protection, 2010. 29: p. 300-305.**

22. **Donald H. Atha, H.W., Elijah J. Petersen, Danielle Cleveland, R. David Holbrook, Pawel Jaruga, Miral Dizdaroglu, Baoshan Xing and Bryant C. Nelson, *Copper Oxide Nanoparticle Mediated DNA Damage in Terrestrial Plant Models.* Environ. Sci. Technol, 2012. 46: p. 1819–1827.**

23. **Ann Cuypers, E.K., Sacha Bohler, Marijke Jozefczak, Kelly Opdenakker, Heidi Gielen, Hanne Vercampt, An Bielen, Kerim Schellingen, Jaco Vangronsveld, and Tony Remans, *Cadmium and Copper Stress Induce a Cellular Oxidative Challenge Leading to Damage Versus Signalling*, in *Metal Toxicity in Plants: Perception, Signaling and Remediation*, D.K.G.a.L.M. Sandalio, Editor. 2012, Springer-Verlag: Berlin. p. 65-90.**

24. **B.Sun, F.J.Z., E. Lombi and S.P. McGrath, *Leaching of heavy metals from contaminated soils using EDTA.* Environmental Pollution, 2001. 113: p. 111-120.**

25. **Zhao, Y.X.a.D., *Removal of Copper from Contaminated Soil by Use of Poly(amidoamine) dendrimers.* Environmental Sci. Technol, 2005. 39: p. 2369-2375.**

26. **John D. Morton, K.F.H., and Jeremy D. Semrau, *Bioavailability of Chelated and Soil-Adsorbed Copper to Methylosinus trichosporium OB3b.* Environ. Sci Technol, 2000. 34(23): p. 4917-4922.**

27. **Xu Song, F.L., Jingwei Ma, Nengqin Jia, Jianming Xu & Hebai Shen, *Synthesis of Fluorescent Silica Nanoparticles and Their Applications as Fluorescence Probes.* Journal of Flourescence, 2011. 21: p. 1205–1212.**

28. **M. Schmidt , F.S., *Applications for silica aerogel products.* Journal of Non-Crystalline Solids, 1998. 225: p. 364–368.**

29. **Liane M. Rossi, L.S., Frank H. Quina, and Zeev Rosenzweig, *Stober Synthesis of Monodispersed Luminescent Silica Nanoparticles for Bioanalytical Assays.* Langmuir, 2005. 21: p. 4277-4280.**

30. **Maniprasad, P.a.S.S., *Novel Copper (Cu) Loaded Core-Shell Silica Nanoparticles with Improved Cu Bioavailability: Synthesis, Characterization and Study of Antibacterial Properties.* Journal of Biomedical Nanotechnology, 2012. 8(4): p. 558-566.**

31. **Christophe Santo, E.W.L., Christian G. Elowsky, Davide Quaranta, Dylan W. Domaille Christopher J. Chang and Gregor Grass, *Bacterial Killing by Dry Metallic Copper Surfaces.* Applied and Environmental Microbiology, 2011. 77(3): p. 794-802.**

32. **Cindy Gunawan, W.Y.T., Christopher P.Marquis and Rose Amal, *Cytotoxic Origin of Copper(II) Oxide Nanoparticles: Comparative Studies with micron-Sized Particles,Leachate, and Metal Salts* ACS Nano, 2011. 5(9): p. 7214-7225.**

33. **Christophe Santo, P.V.M.a.G.G., *Isolation and Charazterization of Bacteria Resistant to Metallic Copper Surfaces.* Applied and Environmental Microbiology, 2010. 76(5): p. 1341-1348.**

34. **Santra, S., *Silica-Based Antibacterial and Antifungal nanoformulation*, U.S.P. Office, Editor 2012, University of Central Florida Research Foundation,Inc.: U.S.A.**

35. **Fenfang Li, C.L., Qinpeng Shen, Lijun Li, Mong Wang, Manli Guo, Yan Huang, Zhou Nie and Shouzhuo Yao, *Analysis of copper nanoparticles toxicity based on a stress-responsive bacterial biosensor array.* Nanoscale, 2013. 5: p. 653-662.**

36. **V. Brezova, M.V., M. Breza, H.Morris, J.Telser, D.Dvoranova, K.Kaiserova, L.Varecka, M.Mazur, and D.Leifritz, *Role of Radicals and Singlet Oxygen in Photoactivated DNA Cleavage by the Anticancer Drug Camptothecin: An Electron Paramagnetic Resonance Study.* Journal of Physical Chem., 2003. 107(10): p. 2415-2425.**

37. **B.G Stephens, H.L.F.J.a.W.M.S., *Spectrophotometric Determination of Copper and Iron Subsequent to the Simultaneous Extraction of Bis(2,9-dimethyl-1,10-phenanthroline)copper(I) and Bis(2,4,6-tri(2-pyridyl)-1,3,5-triazine)iron(II) into Propylene Carbonate.* Analytical Chemistry, 1974. 46(6): p. 692-696.**

38. **Hsue-Yin Hsu, S.-F.T., Kai-Wei Lin, Shyh-Chyun and Chun-Nan Lin, *Cell Death induced by flavonoid glycosides with and without copper.* Food and Chemical Toxicology, 2008. 46: p. 2394-2401.**

39. **Burcu Bekdeser, M.O., Kubilay Guclu and Resat Apak, *Novel spectrascopic sensor for the hydroxyl radical scavening activity measurement of biological samples.* Talanta, 2012. 99: p. 689-696.**

40. **Shiva K. Rastogi, V.J.R., CharLene Gibson, David A. Newcombe, Josh R. Branen and A. Larry Branen, *Ag colloids and Ag clusters over EDAPTMS-coated silica nanoparticles: synthesis, characterization, and antibacterial activity against Escherichia coli.* Nanomedicine: Nanotechnology, Biology, and Medicine, 2011. 7: p. 305–314.**

41. **Institute, C.a.L.S., *Methods for Dilution Antimicrobial Susceptibility Tests for Bacteria That Grow Aerobically;Approved Standard-Ninth Edition*, in *CLSI Document M07-A9*2012, Clinical and Laboratory Standards Institute: Wayne, PA.**

42. **Bo Shen, R.G.J.a.H.J.B., *Mannitol Protects against Oxidation by Hydroxyl Radicals.* Plant Physiol., 1997. 115: p. 527-532.**

43. **N.E.Cameron, Z.T., L.McCabe and M.A.Cotter,** ***Effects of the hydroxyl radical scavenger, dimethylthiourea, on periferal nerve tissue perfusion, conduction velocity and nociception in experimental diabetes.*** **Diabetologia, 2001. 44: p. 1161-1169.**

44. **Haim Shirin, H.A., Avi Alin, Zipora Matas, Michal Kirchner, Eli Brazowski, Ilana Goldiner, Rafael Bruck,** ***Inhibition of Immune-Mediated Concanavalin A-Induced Liver Damage by Free-Radical Scavengers.*** **Digestive Diseases and Sciences, 2009. 55(2): p. 268-275.**